

UNCLASSIFIED

AD 4 2 3 7 3 9

DEFENSE DOCUMENTATION CENTER

FOR

SCIENTIFIC AND TECHNICAL INFORMATION

CAMERON STATION, ALEXANDRIA, VIRGINIA



UNCLASSIFIED

NOTICE: When government or other drawings, specifications or other data are used for any purpose other than in connection with a definitely related government procurement operation, the U. S. Government thereby incurs no responsibility, nor any obligation whatsoever; and the fact that the Government may have formulated, furnished, or in any way supplied the said drawings, specifications, or other data is not to be regarded by implication or otherwise as in any manner licensing the holder or any other person or corporation, or conveying any rights or permission to manufacture, use or sell any patented invention that may in any way be related thereto.

423339

AFSWC TDR 63-47

SWC
TDR
63-47

EXPERIMENTAL STUDY OF THE EFFECT OF MATERIAL
PROPERTIES ON COUPLING OF EXPLOSION ENERGY

TECHNICAL DOCUMENTARY REPORT NUMBER AFSWC TDR 63-47

May 1963



Research Directorate
AIR FORCE SPECIAL WEAPONS CENTER
Air Force Systems Command
Kirtland Air Force Base
New Mexico

Project Number 1080, Task Number 108001

This research has been funded by the Defense
Atomic Support Agency under WEB No. 14.145

(Prepared under Contract AF 29(601)-5360 by
Kenneth Kaplan, United Research Services,
Formerly Broadview Research Corporation,
1811 Trousdale Drive, Burlingame, Calif)

HEADQUARTERS
AIR FORCE SPECIAL WEAPONS CENTER
Air Force Systems Command
Kirtland Air Force Base
New Mexico

When Government drawings, specifications, or other data are used for any purpose other than in connection with a definitely related Government procurement operation, the United States Government thereby incurs no responsibility nor any obligation whatsoever; and the fact that the Government may have formulated, furnished, or in any way supplied the said drawings, specifications, or other data, is not to be regarded by implication or otherwise as in any manner licensing the holder or any other person or corporation, or conveying any rights or permission to manufacture, use, or sell any patented invention that may in any way be related thereto.

This report is made available for study upon the understanding that the Government's proprietary interests in and relating thereto shall not be impaired. In case of apparent conflict between the Government's proprietary interests and those of others, notify the Staff Judge Advocate, Air Force Systems Command, Andrews AF Base, Washington 25, DC.

This report is published for the exchange and stimulation of ideas; it does not necessarily express the intent or policy of any higher headquarters.

Qualified requesters may obtain copies of this report from DDC. Orders will be expedited if placed through the librarian or other staff member designated to request and receive documents from DDC.

FOREWORD

This work was done by the Burlingame Research Center of URS under the administration of Mr. A. B. Willoughby, General Manager. Mr. K. Kaplan, the author of the report, served as Project Manager. Messrs. V. W. Davis, J. Edmunds and J. Boyes participated in much of the material preparation and explosive testing; Messrs. D. Walters and C. Wilton performed additional data reduction; and Mr. O. Criner aided in the analysis of the mounting system. The purpose and basic approach were conceived by Mr. Harold R. J. Walsh, of the Air Force Special Weapons Center; he and Mr. Frederick H. Peterson served as project engineers for AFSWC on this program.

This report is further identified by the Contractor's Report Number URS 609-11.


ABSTRACT


An experimental study was made of the influence of material properties of the directly transmitted effects on explosions. Small spherical high-explosive charges were used to load a series of cylindrical blocks of fine aggregate concrete, either at the surface of a block, within a block, or at the contact surface of two blocks. Measurements were made of the variations in concrete properties, of the total impulse delivered to the block supports, of the permanent deformations and craters, and of the air-blast pressures. It was found that material properties have a major effect on the total impulse transmitted to the material, little effect on the air blast waves, and a very large influence on the sizes and shapes of the craters produced. Although crater dimensions appeared to vary approximately as the cube root of charge weight, both the crater volume and the total impulse varied by at least a factor of two, and scaled crater depth appeared to be approximately independent of burst geometry. The compressibility, as measured by Young's modulus, appeared to have greatest effect on the impulse, while the internal shear strength and other properties reflecting the internal structure of the material had greatest effect on crater dimensions.

PUBLICATION REVIEW

This report has been reviewed and is approved.


FREDERICK H. PETERSON
Project Engineer


HAROLD R. J. WALSH
Project Engineer


THOMAS J. LOWRY, JR.
Colonel USAF
Chief, Structures Branch

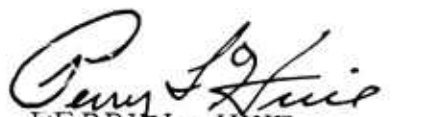

PERRY L. HUIE
Colonel USAF
Chief, Research Division

TABLE OF CONTENTS

<u>Section</u>		<u>Page</u>
1	INTRODUCTION	1
2	PROGRAM DESIGN	3
	Materials	3
	Test Material Constituents	4
	Mix Designs	6
	Material Preparation	7
	Material Property Tests	10
	Test Design	13
	Charge Size and Geometry	13
	Test Sample Geometry	14
	Test Sample Size	16
	Transient Effects Measurements	21
	Permanent Effects Measurements	27
	Test Plan	28
3	TEST RESULTS	31
	Material Property Tests	32
	Measuring Systems: - Operation and Interpretation	35
	Total Impulse System	35
	Air Impulse Measuring System	39
	Surface Burst Geometry Tests	41

Table of Contents (Cont'd)

<u>Section</u>		<u>Page</u>
3	Continued	
	Impulse Measurements	41
	Energy Measurements	48
	Crater Measurements	48
	Split Sample Geometry Tests	53
	Impulse Measurements	57
	Crater Measurements	57
	Totally Contained Geometry Tests	60
4	CONCLUSIONS	65
	REFERENCES	67
	APPENDIX	68
	Tabulated Load Cell and Air Pressure Gauge Data	
	DISTRIBUTION	73

LIST OF FIGURES

<u>Number</u>		<u>Page</u>
1	Mortar Mixer, Mortar Saw, and Foam Generator and Nozzle	9
2	Compressometer-Extensometer for use with 4-inch Diameter, 8-inch Long Cylindrical Specimens	9
3	Photographs from Preliminary Tests with 27-Gram Spherical Charges	18
4	Photograph of the Final Result of a Preliminary Test with a 0.8-inch Diameter Charge in a Split-Sample Geometry	20
5	Mold Face Plates and Charge Hole Hemispheres	20
6	Explosion Test Facility at URS Field Site	25
7	Load Cell	25
8	Typical Oscillograph Records	38
9	Free-Air Shock Wave Peak Pressure Versus Distance d Divided by Cube Root of Charge Weight Y ,	40
10	Free-Air Shock Wave Side-On Impulse per Unit Area I Divided by Cube Root of Charge Weight Y Versus Distance in Charge Radii	42
11	Typical Air Pressure Gauge Traces	43

List of Figures (Cont'd)

<u>Number</u>		<u>Page</u>
12	Impulse I_T and Impulse I_T Divided by Charge Weight Y Versus Young's Modulus .	47
13	Craters from Surface Burst in High Com- pressive Strength 20-inch Diameter Blocks	49
14	Craters from Surface Burst in High Compressive Strength and Low Com- pressive Strength Blocks of Mixes Containing Pumice Aggregate	50
15	Crater Volumes from Surface Bursts on 20-inch Diameter Blocks Versus the Inverse of the Product of Bulk and Internal Shear Strength	54
16	Frames from Motion Picture Record of a Split-Sample Geometry Test	56
17	Craters in Split-Sample Geometry Blocks .	58
18	Craters in Split-Sample Geometry Blocks .	59
19	Frames from Motion Picture Record of First Totally Contained Geometry Test .	61
20	Frames from Motion Picture Record of Second Totally Contained Geometry Text	64

LIST OF TABLES

<u>Number</u>		<u>Page</u>
1	Final Mix Designs	8
2	Explosive Charge Dimensions	15
3	Test Identification Numbers	29
4	Identification of Mixes	30
5	Material Property Test Results	33
6	Impulse Measurements and Calculations . .	44
7	Impulse Measurements and Calculations . .	45
8	Crater Measurements	51
9	Crater Measurements	52
10	Impulse and Crater Measurements	55
11	Cavity Dimensions	62

Section 1

INTRODUCTION

Although many tests have been made to determine various effects of explosions in and on rocks, in very few cases were the influence of material properties either controlled or measured except in the grossest sense. It is known, however that rocks exhibit a wide range of mechanical and structural properties, so large a range, in fact, that explosive energy transfer mechanisms must be affected.

The purpose of the research conducted by United Research Services for the Air Force Special Weapons Center under Contract AF 29(601)-5360 was to attempt to find correlations between the properties of rock-like materials and various measures (e.g. impulse and crater size) of the coupling of explosion energy to these materials.

The basic approach chosen was a straightforward one: Blocks of rock-like materials with widely varying material properties were to be subjected to explosive energy releases of varying sizes. Measurements were to be made of a number of properties of the block material, of the total impulse delivered into the block directly from the explosion, and of the dimensions of the craters and the patterns of near-crater cracking and compaction produced. Block geometries were to be chosen to provide for some to be loaded by a surface explosion, others a contained explosion.

In the course of the investigation, criteria were established and techniques devised for preparing these materials, for monitoring the material properties, for exposing samples of the material to explosive loads, and finally, for measuring the effects of the explosive loads. In Section 2 of this report, the accomplishment of these tasks, i.e. the design of the testing program, is described. In Section 3 of the report, the results of the program are presented.

Section 2

PROGRAM DESIGN

MATERIALS

Ideally, the materials for this program should exhibit properties similar to those of naturally occurring rocks that could be varied independently and at will over any range thought to be of interest.

Certain properties of rock, such as compressive strength and density obviously have a great effect on the coupling of explosion energy. Other properties, such as nonuniformity and nonisotropy, represent complex combinations of simpler properties, and their study should be delayed until better understanding of the influence of the latter is achieved. In this program, therefore, test materials were prepared that were as uniform¹ and as isotropic as possible and that exhibited other properties thought to be of importance to the energy coupling problem over ranges naturally occurring in rock.

The desirability of achieving independent variations in these properties (so that the effects of each could be evaluated separately) is clear, but the actual achievement of this goal is difficult. The test materials prepared in this program consisted of cement mortars and pastes. The chemical processes that occur in the solidification of such materials are highly complex (and in some details still not at all well understood). In the process of solidification, certain properties of the materials appear to become interdependent. However, a few important properties, notably compressive strength and bulk density, can to a degree, be controlled and varied independently by proper choice of constituents.

-
1. Uniformity is used here in the sense that the properties were not functions of gross position within the material.

Test material constituents. Portland cement has had such long use as a constituent in structural concretes that compressive strengths of the concretes can be predicted fairly well. Therefore, portland cement pastes were used as the cementing substance.

To achieve as much uniformity as possible, and yet have control of bulk density, fine grained aggregates of various specific gravities were used as filler material. Thus, our test materials were mortars of various kinds.

Initially, engineers from a local concrete-testing laboratory were consulted for advice on choice of constituents and mix design. At that stage of the program, the following material design specifications had been established: The mortars used would contain aggregates of three different specific gravities (so that the bulk densities of the mortars would be varied) and would differ in strength and compressibility. Nine mixes were to be used, three with each aggregate: a high strength, low compressibility mix; a low strength, low compressibility mix; and a low strength, high compressibility mix. The variations in strength were to be achieved by varying the water-cement ratio and the variations in compressibility, by increasing the volume of the voids in the solidified mix.

One of the three aggregates to be used in the mortars could be readily specified, Ottawa standard sand (American Society for Testing and Materials (ASTM) designation C-190, 20-30 mesh, 2.63 specific gravity). Because this material is used in standard tests for strengths of hydraulic cement mortars, it is readily available, and high standards of uniformity of particle size are maintained.

Specifying properties of the remaining two aggregates was more difficult. A fairly wide range of test material bulk densities and, therefore, of aggregate specific gravities was desired, but there were no other guides to aid us in deciding which particular aggregates should be used.

We first tried to obtain a lighter aggregate than the Ottawa sand to prepare a test material with a lower specific gravity than could be prepared with the sand. On the recommendation of the testing laboratory engineers, the first material tried was an expanded shale, basalite sand. A quantity of more or less standard basalite sand was acquired, which had an apparent specific gravity suitably less than that of the Ottawa sand, but which contained a large proportion of particles considerably larger than could pass a number 20 (841-micron) sieve, the upper limit of the particle size range of the Ottawa sand. The sand was therefore sieved, and much smaller amount (approximately 20 percent of the total) that would pass a number 20 sieve but be retained on a number 30 (595-micron) sieve was obtained. The sieved material was employed in the first mixes, which were designed by the concrete-testing laboratory, for the program.

Unfortunately, it was quickly discovered that the lighter fractions of the basalite sand were discarded along with the large sized particles, and that the specific gravity of the remaining 20-30 mesh portion of the sand was 2.37. This was not sufficiently different from the 2.63 specific gravity of Ottawa sand to produce test materials of significantly different densities, and the basalite sand was rejected for use as an aggregate.

Vermiculite was also tried but rejected. It is readily available and is suitably light in weight, but the individual grains of the varieties that can easily be obtained are relatively large. Grinding or crushing would have been required for it to be usable.

Finally, a source of pumice with a very low specific gravity (less than one) and with an adequately small size range (20-40 mesh) was found. A quantity large enough for the entire testing program was ordered and delivered after an unexpected delay of one month. This material has proven quite satisfactory.

The third aggregate sought was one that was either heavier than Ottawa sand or lighter than pumice. Fine-grained aggregates of the first variety were not readily

available, and it was decided to utilize an aggregate lighter than pumice. The "aggregate" chosen was air, i.e. we sought to incorporate into our cement-water pastes, minute air bubbles in place of particles of an inert solid aggregate.

This was a logical extension of the use of pumice, which has a low specific gravity because of air inclusion in the pumice grains. In addition, a cement-water-air mix should be as uniform or more uniform than a cement-water-pumice (including air) mix. Perhaps the most appealing feature of the use of air without any additional aggregate, however, was the fact that its use would considerably increase the range of compressibilities of the test materials.

A variety of techniques is available for incorporating air (or other gases) into concrete during the mixing process. These include chemical processes in which gas bubbles are produced by the chemical reaction of various substances with the concrete constituents, high-speed mixing in which air is entrained in much the same manner as it is in the preparation of whipped cream, and blending in an already prepared aqueous foam. The last technique is the simplest and easiest to control of the three and was, therefore, chosen for the program.

Accordingly, a foam generator made specifically for producing lightweight, insulating, cellular concrete was acquired.¹

Mix Designs. As noted earlier, in the initial stages of the program mix designs were prepared by a local concrete-testing laboratory. These early designs tended to be less workable than could be tolerated, and each mix exhibited a fairly wide range of compressive strengths that were higher than had been specified. Because of these factors, subsequent designs were prepared at URS.

1. Mearl Chemical Corporation Model 07-10-5B.

The final mix designs were arrived at as a result of experience gained during mixing, casting, and testing materials for the preliminary explosion test series described later in the report. These designs are shown in table 1.

Material preparation. To prepare the materials and samples for tests, a portion of our laboratory space was converted to a storage, batching, casting, and curing facility. A 1,000-pound capacity scale and a 3-cubic-foot mortar mixer were acquired. Ramps were fabricated and installed to facilitate batching and casting. Four water tanks, 5 feet by 2 feet by 2 feet were acquired and equipped with thermostatically controlled heaters to ensure uniform curing. In addition, because sample blocks were to weigh up to 300 pounds, a swinging "I" beam equipped with traveling trolley and chain hoist was fabricated and installed, and small block-handling skids were manufactured. A part of the area set aside for this program is shown in figure 1. Visible are the mortar mixer on a raised platform, the foam generator, and in the background, a mortar saw.

In mixing the materials, ASTM method C305-59T "Mechanical Mixing of Cement Paste and Mortars of Plastic Consistency" was referred to as a guide (Reference 1). Changes consistent with the objectives of the ASTM method were made in the details of the procedure because of the large quantities of materials used, and in the interest of economy. (For example, a commercially available mortar mixer was used instead of one with stainless steel paddles.) The order in which the constituents were incorporated in the mix was the same as in the ASTM method, however, and the mixer used imparted both revolving and axial motion to the constituents.

For casting the test samples, the mixed mortar was shovelled into previously prepared molds, and continuously vibrated with a standard concrete vibrator during the casting process.

The planned curing cycle of the test materials was as follows: After casting, the materials, still in their molds, were to be allowed to cure in the air for one day for an

Table 1

FINAL MIX DESIGNS
Proportions by Weight
(Air in Time of Foam Generator Operation)

<u>Mix Number</u>	<u>Cement¹</u>	<u>Water</u>	<u>Sand²</u>	<u>Pumice³</u>	<u>Air (seconds)</u>
1	1	0.388	2.05		
2	1	.445	2.05		
3	1	.438	2.13		4.1
4	1	.545(0.281) ⁴		0.51	
5	1	.636(0.381) ⁴		0.51	
6	1	.722(0.438) ⁵		0.71	4.1
7	1	.347			2.1
8	1	.351			4.0
9	1	0.351			5.0

-
1. Permanent Type 1. Specific gravity = 3.15
 2. Ottawa standard 20-30 mesh sand. Specific gravity = 2.63
 3. Pumice 20-40 mech. Specific gravity = 0.88
 4. 50 percent of pumice weight of water was required to bring pumice to saturated surface dry condition
 5. 40 percent of pumice weight of water was required to bring pumice to saturated surface dry condition

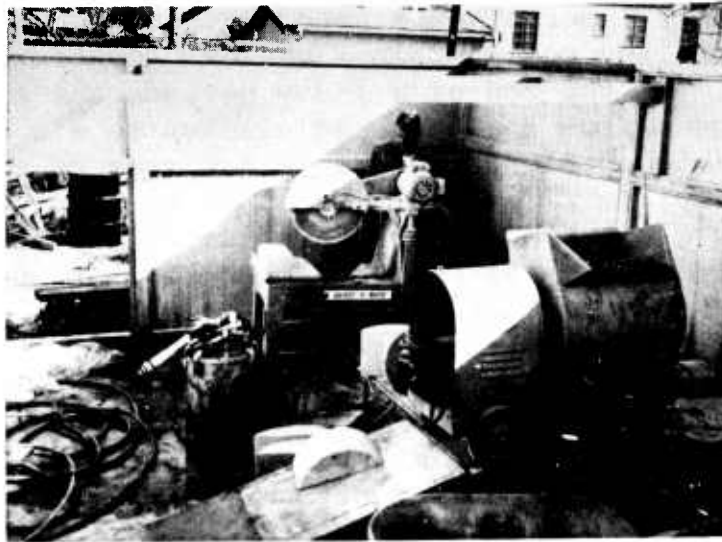


Figure 1

MORTAR MIXER, MORTAR SAW, AND FOAM GENERATOR AND NOZZLE

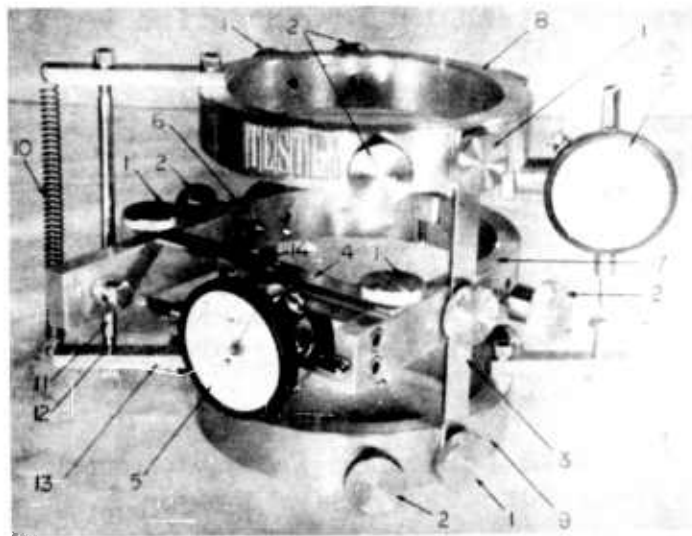


Figure 2

COMPRESSOMETER-EXTENSOMETER FOR USE WITH 4-INCH DIAMETER,
8-INCH LONG CYLINDRICAL SPECIMENS

initial set. The molds were then to be removed, and the samples completely immersed in a water bath that was thermostatically controlled to maintain a uniform temperature of 72° Fahrenheit. At the end of a 7-day period, the samples were to be removed from the bath and allowed to air cure for an additional 7-day period. Delays in delivery of other test equipment¹ did not permit strict adherence to this uniform 15-day curing cycle. However, all samples of any one mix were subjected to identical curing cycles so that uniformity within each mix type was maintained.

Material property tests. In the course of the study, tests were conducted to monitor the following properties: compressive strength, tensile strength, bulk density (just before explosion tests), water content (just before explosion tests), Young's modulus, and Poisson's ratio. In addition, calculations were made of air void volume (just before explosion tests), of the internal shear strength, and of the shear and bulk moduli. Wherever available, standardized procedures were followed. A description of the tests and calculations made to determine these properties follows.

Compressive strength. Compression test specimens were prepared in general accord with ASTM method C31-59 for making and curing concrete specimens in the field. This procedure was followed instead of that of ASTM method C192-59 for preparing specimens in the laboratory because it was desired that test specimens be as much like the material cast for explosion tests as possible. Accordingly, specimens were cast into cylindrical, paraffined-cardboard molds 4 inches in diameter and 8 inches long, and vibrated and cured in the same manner as the samples cast for the explosion tests.

The tests were performed in accord with ASTM method of test C39-61 for compressive strength of molded

-
1. Delivery schedules of explosive charges, a compressor-extensometer, and of the basic spring mount system were not met.

concrete cylinders, at a local concrete-testing laboratory. A minimum of two specimens per mix was tested.

Tensile strength. Specimens were prepared and tests conducted in accord with ASTM standard method of test C190-59 for tensile strength of hydraulic cement mortars, except, of course, that the specimens contained the aggregates used in the design mixes instead of the standard aggregate specified in the test procedure.

Bulk density. These densities were obtained on explosion test days by weighing in air and water specially prepared 2-inch diameter, 4-inch long specimens cast and cured at the same times as the other specimens and samples.

Water content. The amount of water that was used in preparing the samples was known, but the portion that was free and unreacted could not be determined at the time of explosion tests from measurements of weight loss alone. Instead, test specimens were weighed at shot date, and then placed in an oven for drying. When weight loss due to drying ceased, the specimens were weighed again, and the difference in weights was the approximate free water content at the time of explosion. Such a measurement can only be approximate, however, because during the drying period, a limited amount of water continued to react with the cement.

Young's modulus. Measurements of Young's modulus were made by the local testing laboratory in accord with ASTM tentative method of test C469-61T. This test and that for Poisson's ratio required the fabrication of a special compressometer-extensometer, whose basic design elements are given in C-469-61T. A photograph of the device is shown on figure 2.

Poisson's ratio. ASTM tentative method of test C-469-61T also deals with standard test procedures to determine Poisson's ratio. The same compressometer-extensometer employed in the Young's modulus tests was used for determining lateral displacements required to compute this quantity. The extensometer part of the instrument, as initially delivered

was not in complete accord with the details of the design given in C-469-61T. With the proper conversion factors, however, the instrument could be used for its intended purpose.

Air void volume. Calculations of air void volume were made from the results of weighings made on the date of the explosion tests and from knowledge of the quantities of water and other constituents used in preparing the mixes initially. Any loss in weight during the time between casting and explosion tests could only be of free water, and the volume of the water lost closely represents the volume of the air voids in the test specimens.

Internal shear strength. Calculations of internal shear strength were made by an adaptation of the method employing Mohr's circles for compressive and tensile strength outlined in reference 2. From that method, the following formula can be derived:

$$\tau_s = \frac{\sigma_c}{2} \sqrt{1 - \left(\frac{\sigma_c - \sigma_t}{\sigma_c + \sigma_t} \right)^2} \quad (1)$$

where τ_s = shear strength

σ_c = compressive strength

σ_t = tensile strength

Shear and bulk moduli. These values were calculated with the following relationships from elastic theory:

$$\text{shear moduli} = E_s = \frac{E}{2(1 + \nu)} \quad (2)$$

$$\text{bulk moduli} = E_B = \frac{E}{3(1 - 2\nu)} \quad (3)$$

where E = Young's modulus

ν = Poisson's ratio

TEST DESIGN

The testing under this contract had the specific objective of providing information on the influence of material properties in the coupling of explosion energy to rock-like materials. This was to be done by: monitoring dynamic reactions of samples of the various materials, and by acquiring information on the differences in the craters formed by charges placed on a free surface of the materials and charges completely contained in the materials. In the following, interrelated aspects of explosive design and test sample design are first discussed, after which the design of the instrumentation used to accomplish the stated objective is described.

Charge size and geometry. At the outset, little information was available that would guide us in determining the sizes of explosives that could be used with various sizes and configurations of test samples. Such information is quite critical in determining the costs of the tests performed since they determine the quantity of materials used for the tests and the ease with which test samples can be handled. The relatively few data in the literature, e.g. reference 3, indicated that small quantities of explosives, on the order of a few grams, would be required to prevent prohibitive handling and material costs. These data indicated that tests using 8-gram charges might require samples with free surface diameters of as much as 16 inches. By extension, tests with charges 50 percent greater in size could require samples whose dimensions were 50 percent greater in size, or a free surface diameter of 2 feet. Even with the hemispherical samples (which were initially planned for use), an individual test block could weigh as much as 300 pounds.

This gross size range was close to the limit of sizes and weights of individual blocks that could be handled simply, and therefore, an upper limit on charge size was established at approximately 27 grams. [A charge 1.5 times the size of an 8-gram charge would weigh $(1.5)^3$ times 8 grams, or 27 grams.]

Centrally detonated spherical charges were clearly indicated because of the uniformity of the stress and shock waves generated. Because a wide range of energy releases also appeared desirable, the basic charge size range was established (somewhat arbitrarily) at 50 percent larger and 50 percent smaller than that of 8-gram charges (~0.8 inches in diameter). Accordingly, centrally detonated spherical explosive charges 0.4, 0.8, and 1.2 inches in diameter were ordered.¹ The actual quantities of explosives contained in these charges (which consist of a lead azide core surrounded by blankets of various explosives) were 0.90, 7.09, and 24.28 grams. As a result of tests that took place late in the program (which are described later in this report), additional charges 0.6 inch in diameter were also used. The constituents and dimensions of the charges used in this program are shown in table 2.

Test sample geometry. The basic sample geometries of concern in this program are one in which the spherical charge is located at the surface of a sample block (i.e. half in half out of the material), and one in which the charge is totally contained within the sample material. The latter geometry does not permit meaningful dynamic measurements of block response. A third configuration, termed a split-sample geometry, was also employed. In this geometry, the charge was placed in a hole between the faces of two closely fitting blocks. When detonation occurred, the blocks, not being joined in any way normal to these flat faces, could move along the normal. Hopefully, the crater- or cavity-producing mechanisms in this geometry resembled the mechanisms in the totally contained geometry, yet the reactions of the individual halves of the sample could be measured.

Initially we proposed casting hemispherical blocks for the surface and split-sample geometry tests and spherical blocks for the totally contained geometry tests.

-
1. The charge manufacturer is Maryland Assemblies, Incorporated, of Port Deposit, Maryland.

Table 2
EXPLOSIVE CHARGE DIMENSIONS
(Inches)

<u>Charge Diameter</u>	<u>Lead Azide Core Diameter</u>	<u>Pentolite Blanket Thickness</u>
0.4	0.150	0.250
0.6	.312	.288
0.8	.312	.488 ¹
1.2	0.312	0.888

-
1. An initial order placed for 0.8-inch diameter charges specified a 0.150-inch diameter lead azide core surrounded by a 0.162-inch thick blanket of CH-6, surrounded by another 0.488-inch thick blanket of pentolite. The CH-6 was discovered by the manufacturer to be faulty before the explosives were used, and the charges revised as shown were ordered.

While a hemisphere would be the ideal geometry to use for both the surface and split-sample geometry tests, difficulty would have been encountered in finishing the flat surfaces of the hemispheres to sufficiently close tolerances for the split-sample geometry tests. Therefore, an alternative to the hemispherical shape was sought.

In preliminary tests with explosive charges (made to gather information on block sizes), blocks that were rectangular in plan and section were employed. These showed tendencies to crack through the position of the charge to points in the center of the sides normal to the face on which the charge was placed. Clearly, in the rectangular geometry, lines of unacceptably high stress concentration formed. This particular problem could be solved, however, by employing blocks with plane, circular faces on which to place charges. Further examination of the results of the preliminary tests indicated that if the blocks could be made deep enough normal to the charge face, a cylindrical geometry could be employed. The planes and surfaces of stress concentration beneath the charge would be located far enough from the charge to prevent block rupture.

With the cylindrical geometry, blocks could be readily cast with their charge surfaces down (which could not be done with a hemispherical geometry). The mold facing employed for the charge surface, and therefore, the charge surface itself, could then be made to have a finish and detail acceptable for split-sample geometry tests. For such tests, it was deemed desirable to key the surfaces of the two blocks to delay escape of charge detonation products.

Test sample size. As previously indicated, a program of preliminary, largely uninstrumented explosion tests were conducted, in part to provide information on the sizes of test samples or blocks that could be employed with the sizes of charges and the testing geometries contemplated for the major test program. In the first part of this preliminary program, 27-gram spherical charges of Composition A (95% RDX, 5% wax) and 10-gram cylindrical charges of PETN that had been acquired for already completed experimental

programs, were grouted into the square top surfaces of blocks that were half as high as they were wide. Blocks of this type whose dimensions were 6 by 12 by 12 inches, 8 by 16 by 16 inches, and 10 by 20 by 20 inches were employed.¹ Tests were conducted in both surface and split-sample geometries and with both strong and weak mixes.

In the surface shot geometry tests, all of the 6- by 12- by 12-inch and 8- by 16- by 16-inch blocks and the 16-inch diameter hemispherical block ruptured, the smaller ones and the hemisphere shattering into many pieces, the larger ones generally breaking into five or six pieces. With a 10- by 20- by 20-inch, high strength material block, two surface cracks extended through the crater formed by the charge from the center of the opposite sides of the block, but the block remained largely intact. An 8- by 16- by 16-inch block formed a crater but remained otherwise intact when used with a 10-gram cylindrical charge.

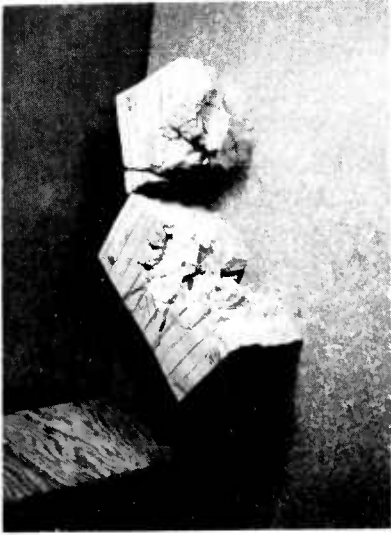
These results suggested that blocks with a charge surface diameter of 16 inches could be used with the 0.8-inch diameter charges, and that blocks with a surface diameter of 20 inches probably could be used with the 1.2-inch diameter charges. Photographs of the results of some of these tests are shown in figure 3.

The split-sample geometry tests were of two types, both employing 0.8-inch diameter charges. In the first type, 10- by 20- by 20-inch rectangular blocks of a strong mix were placed in two swings with charge surfaces vertical and touching; in the second, 20-inch diameter, 12-inch long cylinders of a weak mix were placed one atop the other, with charge surfaces horizontal and touching. The second tests were conducted with the first pours made in the molds that had been designed with keyed, matching bosses. The matched blocks from these molds ideally have raised annuli in one block and depressed annuli in the other, which key

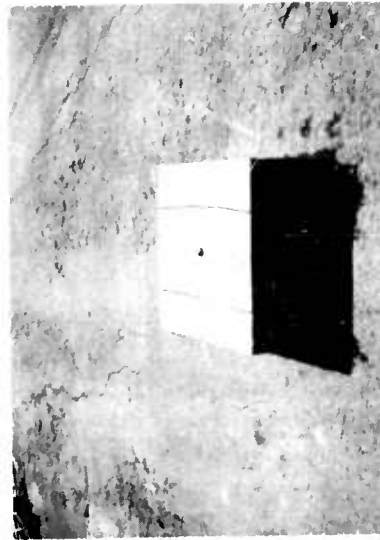
1. A single 16-inch diameter, weak mix, hemispherical block was also tested.



A. Partially Reconstructed Hemispherical
(16-Inch Diameter) Sample



B. Partially Reconstructed Medium-Sized
(8 by 16 by 16 Inches) Sample



C. Large-Sized (10 by 20 by 20 Inches) Sample
Prior to Test (Spherical charge is shown
grouted into the center of the block.)

Figure 3

PHOTOGRAPHS FROM PRELIMINARY TESTS WITH 27-GRAM SPHERICAL CHARGES

together to delay the escape of the high pressure detonation products. In the two blocks used in the preliminary tests, the annuli broke upon removal of the forms, and though the blocks fitted together well, only limited keying of the two was accomplished.

In both tests, the blocks maintained their integrity (except, of course, for the craters that formed about the charge location). A photograph of the results of the second test is shown in figure 4. This result was taken to indicate that matched 20-inch diameter, 12-inch long blocks could be used with 0.8-inch diameter spherical charges in the split-sample geometry. Subsequently, these conclusions proved erroneous, and in tests conducted late in the program, blocks of the same size were employed with newly prepared 0.6-inch diameter spherical charges.

In summary, the results of these preliminary tests indicated that in the surface geometry, 16-inch diameter, 10-inch long cylindrical blocks could be used with 0.8-inch diameter spherical charges and that 20-inch diameter, 12-inch long cylindrical blocks could be used with 1.2-inch diameter spherical charges. In the split sample geometry, the results suggested that 20-inch diameter, 12-inch long keyed and matched blocks could be used with 0.8-inch diameter spherical charges (though they were eventually employed with 0.6-inch diameter spherical charges). Although no preliminary tests were conducted with 0.4-inch diameter charges, because their calculated energy release would be only one-eighth of that of the 0.8-inch diameter charges, keyed and matched blocks 12 inches in diameter and 8 inches long were believed to be adequate.

A picture of the mold face plates for the 20-inch diameter split-sample geometry blocks and for the 16-inch diameter surface geometry blocks is shown in figure 5. The mold bosses are removable so that the 20-inch diameter plates could also be used for casts of 20-inch diameter surface geometry blocks. The plates and bosses are of steel and are centrally tapped for steel hemispheres that form the holes in the test blocks in which charges were placed. The large plates are shown with 0.6-inch diameter

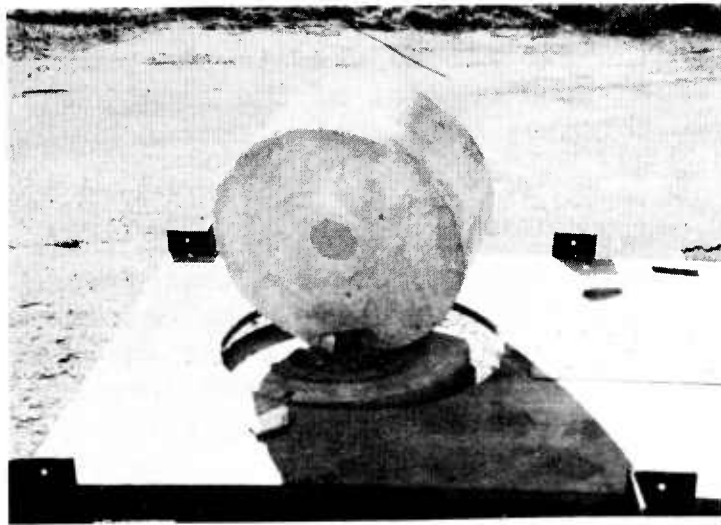


Figure 4

PHOTOGRAPH OF THE FINAL RESULT OF A PRELIMINARY TEST WITH A 0.8-INCH DIAMETER CHARGE IN A SPLIT-SAMPLE GEOMETRY

Note: Blocks are 20 inches in diameter and 12 inches high.



Figure 5

MOLD FACE PLATES AND CHARGE HOLE HEMISPHERES

Notes: The lower plates are 20 inches in diameter; the upper plate is 16 inches in diameter. The hemispheres shown have diameters of 0.6, 0.8, and 1.2 inches.

hemispheres, the smaller plate with a 0.8-inch diameter hemisphere, and atop the smaller plate rests a 1.2-inch diameter hemisphere.

Transient effects measurements. The primary measurements of transient effects (those that dissipate with time) made were: one that would yield the total impulse imparted to the sample blocks by the explosion as well as the total kinetic energy imparted to the blocks; and one that would yield the approximate impulse imparted to the block by the air shock wave that passes over a block after detonation of a charge in a surface geometry.

Total impulse measurements. The impulse-measuring system used consisted of a helical spring mounting upon which the sample blocks were placed. Charges were placed on the upper surface of a block, and upon exploding, imparted a downward force in a direction to compress the springs. The period of response of the system was quite long compared with the time during which force was applied to the top surface of a block. This type of system, which might be termed a soft mounting (as opposed to a hard mounting in which the period of response of the mounting would be very short compared with the loading duration) was chosen as a result of the following analysis.

Considering for simplicity a simple system in which a spring with negligible mass and spring constant k supports a rigid mass M , and assuming that motion is imparted to the mass by a force F that acts for a time t_1 ,¹ it can be shown that the area under the spring force T versus time t curve is:

$$\int T dt = F(t_1 - \frac{1}{a} \sin at_1) \quad (4)$$

if spring force is measured at the time t_1 and:

$$\int T dt = F(t_1 - \frac{2}{a} \sin \frac{at_1}{2} \cos at_2) \quad (5)$$

-
1. The spring force will depend on the actual time history of the applied force, but the general nature of the behavior of such systems is most clearly seen with the simple input pulse assumed.

where $t_2 = t + (2\pi + \frac{t_1}{2})$

and $a^2 = k/M$

if spring force is measured at a time $t_2 > t_1$. In either case, the period τ of the system is $2\pi/a$.

In a hard mounting system, a is large compared with t_1 (or alternatively the period is short compared with the loading duration); the second term of each expression goes to zero, and the integral becomes $F \cdot t_1$, the true area under the load versus time curve.

In a soft mounting system, a is small compared with t_1 (the period is large compared with the loading duration), and the term $\sin at_1$ in each expression becomes nearly at_1 . In equation (4), the integral becomes nearly zero; in equation (5), the integral becomes:

$$\int T dt = Ft_1(1 - \cos at_2) \quad (6)$$

This is equal to the true area under the loading versus time curve if the integration is carried out to a time of $\pi/2a$, i.e. one-quarter the period of the system.

Thus, integration under the spring force versus time curve of a hard mounting system will always yield the correct value of integrated load versus time, but similar integration carried out for a soft mounting system will yield the correct value of integrated load versus time only if integration is carried out to a time equal to one-fourth the period of the system. These statements are tantamount to saying that a hard mounting system is "fast" enough to follow the loading pulse and that a soft mounting system is too slow to follow the loading pulse, but will eventually respond to the pulse long after loading has terminated.

Clearly, a hard mounting system would yield more information about the loading pulse from spring force versus time measurements. Unfortunately, for the case at hand, the loading durations are so short that provision of a truly

hard system would be difficult if not impossible. As a practical matter, the mounting would probably be made of steel and the sample blocks are far from rigid, i.e. stress pulses do not propagate at infinite velocity within them. Times for passage of stress waves through the materials, added to the times for passage of the waves through the steel can be shown to be of the same order as the expected loading durations of approximately 0.2 millisecond or less.

If the loading duration is as little as one-fourth the period of the system, integrated spring force versus time values carried out to the time of cessation of loading can differ by over 60 percent from the correct integrated load versus time. [See equation (4) with $(1/4)(2\pi/a)$ substituted for t_1 .] Spring force values at the particular time would equal the loading force F but at earlier times would also differ by large percentages (100 percent at the start of the loading pulse). Thus, the "semihard" mounting system just described would offer no advantage at all over a soft-mounting system, and could only be used as would a soft-mounting system, i.e. with measurements of spring force made after the loading pulse had terminated.

The spring mounting system finally adopted was designed to be quite soft in that the period of the system was specified to be not less than about 500 times the estimated loading duration for surface bursts. (The loading duration for split-sample geometries could not be readily estimated).

The maximum spring forces that the system would be subjected to could be estimated fairly well for the surface geometries but not for the split-sample geometries. Therefore, during the test described earlier in which two 10- by 20- by 20-inch blocks were placed on swings with charge surfaces touching, high-speed motion picture records were made of the early motions of the blocks, and estimates were made of the impulse imparted to them.

On the basis of these tests, and in an effort to minimize drag forces by limiting motion, a spring system with a total spring constant of approximately 1,500 lb/in. and with a maximum allowable travel of 3 inches was specified.

It was estimated that the spring-force from split-sample geometry tests would not exceed 500 pounds with such a spring system.

For stability, the load was supported by three springs, thus each was to have a spring constant of 500 lb/in.

A picture of the spring mounting, designed to our specifications by a commercial spring manufacturer, is shown in figure 6. The springs have a free length of approximately 17 inches, are made of 13/16-inch thick chrome vanadium wire, and have an outside diameter of 6 inches. The springs are capped top and bottom by 1/2-inch thick steel plates, 22 inches square. The sample blocks were bolted to the top plate (Studs were integrally cast into each block.) and three load cells, one beneath each spring, were fastened between the lower steel plate and the concrete base beneath it. The base, only a portion of which can be seen in the picture in figure 6, is 2-1/2 feet high and 4 feet square. This large base was required to ensure stability of the system under conservatively estimated upward forces exerted by the springs on the base.

The load cells that form an integral part of the impulse measuring system were made to sense both tension and compression loadings, operate smoothly through the point of zero load, and calibrate identically in both tension and compression¹. They are designed for a maximum force of 3,000 pounds in either tension or compression and have a rated sensitivity of approximately 2 millivolts per input volt at maximum design load.

The signals generated by these load cells were recorded on a galvanometer oscillograph equipped with high sensitivity (460 μ a/in.) galvanometers.

1. Lockheed Electronics Company Model WR6-3TC



Figure 6

EXPLOSION TEST FACILITY AT URS FIELD SITE

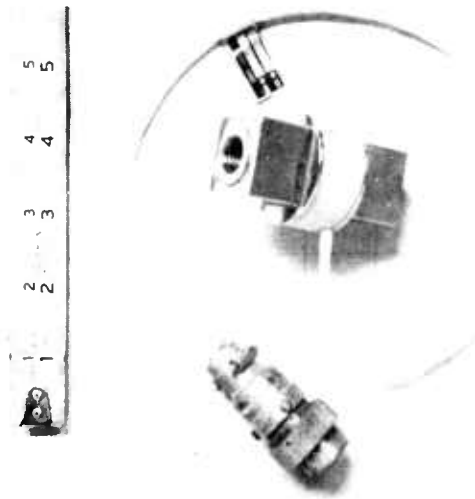


Figure 7

LOAD CELL

Air impulse measurements. No direct measurements of the impulse imparted to the sample blocks solely from passage of air shock waves over their free surfaces could be made. It was conceivable, however, that this impulsive force could represent a significant portion of the total impulse imparted to the blocks by the explosive. Therefore, an indirect method for estimating this impulse was developed.

If it is assumed that the general nature of the air shock's pressure versus distance curve would be little affected by happenings (e.g. crater formation) very near the charge position, but that the energy content of the shock wave would be affected, an air pressure gauge could be used to determine the size of charge that would produce the observed shock. If the assumption made is substantially correct, each gauge in an array of gauges should yield the same value for pseudo charge size from any single test. This charge size could then be used with known experimental and theoretical relationships between side-on impulse and charge size to estimate (approximately) what portion of the total impulse imparted to the block could be ascribed to passage of the air shock wave.

To apply this method, a steel plate 1 inch thick, 8 inches wide, and 24 inches long was drilled and tapped to receive air pressure sensors, and the molds employed for the surface geometries were equipped with a rod that would leave a hole in each block in which a similar sensor could be placed.

The steel plate was placed on a steel legged table of adjustable height. (Height adjustment was necessary because sample blocks of different weights would compress the spring mountings different amounts.) The remainder of the table top was fitted with plywood, the top surface of which was made flush with the steel air pressure gauge plate. A portion of the air pressure gauge plate can be seen in figure 4 and the table, in figure 6.

Block acceleration measurement. In some of the tests, an accelerometer was fastened to the underside of

the upper steel plate of the spring mount. Because of ringing and high noise levels, the output of this gauge could not be interpreted.

Permanent effects measurements. The only measurements made of long-time effects were crater parameters (diameter, depth, and volume). Others were unsuccessfully attempted even though a fair amount of effort was expended in attempting to perform these measurements. We had particularly hoped to monitor permanent displacements of the sample block material caused by explosive loading. For this purpose, we acquired a large (20-inch arbor) mortar saw¹ (See figure 1.) and proceeded to develop techniques for producing fiducial marks within the blocks themselves. In our first attempts, light string and fine wire were integrally cast in certain of the test blocks fired in the preliminary testing program. When these blocks were examined, it was found that, far from serving their intended purpose of monitoring permanent displacements, these foreign materials had acted as reinforcing, and if anything inhibited the production of permanent displacements.

Attempts were then made to place within newly cast blocks filaments of material similar except for color (A dye was added.) to that of the parent blocks. Difficulty was encountered in producing straight filaments and in making them thin enough that displacements of small magnitudes could be seen. The first difficulty was successfully overcome; the second never was. The consistencies of the mortars used, and even of neat cement pastes, preclude their being extruded through long thin tubes as would be necessary for a thin filament.

A few blocks with thick filaments were cast, tested with explosives, and sawed, but no permanent displacements could be found. Thereafter, the technique was abandoned. In figure 5, the spiral of holes leading away from the charge position in the upper charge surface plate were drilled

1. Champion Adjustomatic

specifically for placing the filaments. After abandonment of the technique, these holes were masked with tape to prevent mortar leakage.

TEST PLAN

Material preparation requirements dictated the program schedule. Because we desired all types of tests with each mix to be conducted in blocks with the same properties, all blocks of each mix were to be batched, mixed, and cast on the same day. These were then all to be immersed together, removed together, and tested together. In addition, it was deemed convenient from a storage standpoint to cast and test materials containing the same aggregate sequentially.¹

Special procedures were required to deal with the totally contained geometry blocks. Because these would contain high explosives from the time they were cast, casting could not be done in the Burlingame laboratory. Instead, the scale, mortar mixer, molds, and watering troughs were to be transported to our local field site, far removed from any population centers.

Identification numbers were assigned each test type at the beginning of the program. In all cases, it was planned to conduct duplicate tests of each type and with each material, and the duplicates were assigned the letter designations A and B. Table 3 identifies the tests, and, for convenience, table 4 identifies the character of the mixes.

-
1. These procedures were followed with two exceptions: Test results required recasting of all large split-sample geometry blocks and of the totally contained geometry blocks. These were done in groups of three different mixes toward the end of the test program.

Table 3

TEST IDENTIFICATION NUMBERS

Sample	Charge Diameter (in.)	Mix Number								
		1	2	3	4	5	6	7	8	9
16-inch Surface ¹	0.8	1	5	9	13	17	21	25	29	33
20-Inch Surface ²	1.2	2	6	10	14	18	22	26	30	34
12-Inch Split ³	0.4	3	7	11	15	19	23	27	31	35
20-Inch Split ⁴	0.8	4	8	12	16	20	24	28	32	36
20-Inch Split ⁵	0.6	4'	8'	12'	16'	20'	24'	28'	32'	36'
20-Inch Contained ⁶	0.8	37			38			39		
20-Inch Contained ⁷	0.6	37'			38'			39'		

-
1. 16-inch diameter, 10-inch long block, charge at one flat surface
 2. 20-inch diameter, 12-inch long block, charge at one flat surface
 3. Two 12-inch diameter, 8-inch long blocks, charge between blocks
 4. Two 20-inch diameter, 12-inch long blocks, charge between blocks
 5. Two 20-inch diameter, 12-inch long blocks, charge between blocks
 6. 20-inch diameter, 24-inch long block, charge integrally cast
 7. 20-inch diameter, 24-inch long block, charge integrally cast

Table 4

IDENTIFICATION OF MIXES

<u>Mix Number</u>	<u>Identification</u>
1	High strength Ottawa sand, no foam added
2	Low strength Ottawa sand, no foam added
3	Low strength Ottawa sand, foam added
4	High strength pumice, no foam added
5	Low strength pumice, no foam added
6	Low strength pumice, foam added
7	High strength air, foam added
8	Low strength air, more foam added than for 7
9	Low strength air, more foam added than for 8

Section 3

TEST RESULTS

The testing program successfully achieved many of its goals. The spring mounting-load cell combination operated as anticipated, and yielded good force records as a function of time. The air pressure sensing system also operated satisfactorily. High-speed film records taken during the totally contained geometry tests yielded excellent results. Crater dimensions and volumes were monitored as planned, as were all the material properties described earlier in the report.

Some difficulties, however, were encountered in the test program. Although test blocks were cast for use with the 0.4-inch diameter charges, and experiments with these blocks and charges were conducted in the split-sample geometry, no usable data were obtained from these experiments. The spring force records taken during these tests exhibited extremely wide variations between two shots with identical blocks (up to factors of three). Examination of the test blocks after firing showed a residue--probably of unreacted explosive--that was not present after firings with larger charges.

Another difficulty was encountered (but surmounted) with the split-sample geometry. Two preliminary tests with this geometry, one with 10- by 20- by 20-inch rectangular blocks and one with 20-inch diameter cylindrical blocks, had indicated that blocks of this over-all size would not rupture when 0.8-inch diameter charges were employed. When such tests were conducted, however, with well fitted, matched blocks, they did rupture, in some cases (with the higher strength mixes) into five or six relatively large fragments, in other cases, into many more.

The failure of this particular test condition made it necessary to discard one set of these blocks which had just been removed from the curing bath and another set that was ready for firing.

To continue tests with split-sample geometry blocks required either much larger blocks (to be used with the 0.8-inch diameter charges) or smaller charges (to be used with the 20-inch diameter, 1-foot high blocks). Because of the handling problems that larger blocks would create, the latter course was decided upon. A rush order for 0.6-inch diameter charges (which generate approximately 27/64 the energy that the 0.8-inch diameter charges do) was filled with gratifying speed. Still, because of the 15-day lag between casting the blocks and testing them, and because of the necessity to recast four complete sets of blocks, the testing program was unavoidably delayed.

Finally, as in any extensive testing program, because of mischance, some data points were missed in otherwise successful tests.¹

The results of the material property tests, the general operation of the measuring systems, and the results of the explosion tests are summarized, analyzed, and discussed in the following sections.

The raw results of the explosion tests are presented in tabular form in the appendix to this report.

MATERIAL PROPERTY TESTS

The result of the property tests are presented in tabular form in table 5. It can be seen that wide ranges of properties

-
1. A few missed data from the load cells had a more prosaic cause. The cells contain strain gauges which apparently are subject to creep over a period of months, resulting in a zero shift. Eventually, one drifted beyond the capacity of the oscillograph to correct the shift. This required rebalancing the cells with externally applied resistors, and recalibrating the cell-resistor combination. The drifting phenomenon occurred twice during the tests. We have been informed by the cell manufacturer that the condition is correctable.

Table 5

MATERIAL PROPERTY TEST RESULTS

<u>Mix Number</u>	<u>Compressive Strength (psi)</u>			<u>Tensile Strength (psi)</u>			<u>Bulk Density (pcf)</u>	<u>Air Void Volume (ft³/ft³)</u>
	<u>min</u>	<u>avg</u>	<u>max</u>	<u>min</u>	<u>avg</u>	<u>max</u>		
1	6720	7700	8350	635	670	715	140.0	0.03
2	5400	5400	5400	225	230	235	140.0	.01
3	1150	1155	1160	205	212	220	102.0	.28
4	4550	4660	4700	350	368	390	92.5	.13
5	2610	2780	2950	240	270	300	91.0	.12
6	390	540	685	100	100	100	58.6	.39
7	5500	5730	6120	145	220	230	111.0	.12
8	2600	2730	2860	150	160	170	94.8	.25
9	971	1450	1932	155	158	160	84.8	0.33

Table 5 (Cont'd)

Material Property Test Results

<u>Mix Number</u>	<u>Internal Shear Strength (psi)</u>	<u>Young's Modulus (10⁶ psi)</u>	<u>Poisson's Ratio</u>	<u>Shear Modulus (10⁶ psi)</u>	<u>Bulk Modulus (10⁶ psi)</u>	<u>Free Water (pcf)</u>
1	2100	5.67	0.162	2.43	2.79	8.05
2	1740	4.78	.109	2.16	2.04	9.0
3	422	0.97	.044	0.48	0.36	4.7
4	1213	1.59	.138	0.70	0.73	10.0
5	789	1.33	.118	0.60	0.58	15.7
6	196	0.37	.093	0.17	0.15	12.0 ¹
7	1080	2.02	.115	0.82	0.87	15.5
8	624	1.38	.128	0.61	0.62	15.4
9	432	0.96	0.119	0.43	0.42	14.2 ¹

1. Weight loss had not yet ceased at time of measurement.

were successfully achieved. Most compressive and tensile tests were conducted on two cylindrical compression specimens and two "dogbone" tensile specimens from each mix although for mixes 4 and 7, three samples of each type were used, and for mix 1, eight samples of each type were used. The range of measured values of compressive and tensile strength tests are shown in the table.

MEASURING SYSTEMS - OPERATION AND INTERPRETATION

Total impulse system. Earlier in this report, an analysis of a simple spring mass system was given in which it was shown, assuming the spring to be weightless and the system without damping, that the motion of the mass would be sinusoidal, and that the integral of the spring force versus time curve to the time of maximum spring force would yield the impulse that put the mass into motion. In our spring mounting system, the spring has weight, and the effect of this weight is to modify the basic sinusoidal motion.

One modification comes about in the fundamental mode of the system; the period of oscillation decreases as the ratio of spring weight to supported weight increases. The decrease in period is not, however, enough to modify the basic "softness" of the system, i.e. the basic period of oscillation of the spring mounting is still very long compared with the duration of the loading pulse.

This can be seen by extending an analysis given by Timoshenko (Reference 4) for the longitudinal oscillations of a prismatic bar to which a weight is attached, to the case of a weight on a helical spring. In the spring analysis, the fundamental period T of the spring mass system is given by:

$$T = \frac{2\pi}{p}$$

$$p = \frac{a}{\ell} \cdot \beta \tag{7}$$

$$\beta \tan \beta = \alpha = \frac{w\ell}{W}$$

where l = spring length

k = spring constant

w = weight of spring per unit length

W = weight of the supported mass

g = acceleration due to gravity

$$a = \sqrt{kg l/w}$$

Values of β are given in Timoshenko for various values of α . In our system, the total weight of the free coils of the springs is approximately 56 pounds. The weight supported by the springs, including that of the steel plate upon which the blocks rested and the plugs to which the springs are attached, had a maximum value of approximately 400 pounds and a minimum value of approximately 170 pounds. For the maximum weight, $\alpha = 0.145$, $\beta \approx 0.4$, and the period T becomes ~ 0.15 seconds. For the minimum weight, $\alpha = 0.33$, $\beta = 0.55$, and T becomes approximately 0.11 seconds. (Both values of T are very close to those actually measured for the two cases, viz 0.15 and 0.115 second.)

A second modification of the basic sinusoidal motion caused by the springs having significant weight, is the generation of an oscillation of higher frequency within the springs themselves (a higher mode of the basic system). If this oscillation is of significant amplitude, it can have more serious consequences than the period decrease mentioned above.

It can be shown, by assuming the spring's weight to be concentrated at its center of gravity (in which case there is a double spring, double weight system), that the motion of the spring mass is given by:

$$T = ky_1 = \frac{2kI \sqrt{\frac{kg}{w}}}{W(v^2 - u^2)} \left\{ \frac{\sin ut}{u} = \frac{\sin vt}{v} \right\} \quad (8)$$

where

$$-v^2 + u^2 = \left[\left(\frac{kg}{W} \right)^2 + 4 \left(\frac{kg}{w} \right)^2 \right]^{1/2}$$

and the other variables are as defined earlier.¹

The important thing to note in these equations is that a simple integration to a maximum value of spring force T no longer yields the impulse I directly as it did in the case of the single spring, single mass system. Thus, if the spring oscillations are of significant size, there is no simple procedure for determining input impulse from spring force versus time records.

The records from our spring mounting system show both types of oscillations, as can be seen in the typical record of figure 8. Furthermore, at the outset, the higher frequency oscillations are indeed of significant size. These oscillations, however, attenuate with time, and at the time of the third low frequency oscillation are very small. While viscous damping could account for this attenuation, a more plausible conclusion is that an exchange of energy between the two oscillation frequencies took place with the energy in the higher frequency mode converting to energy in the lower frequency mode. (See Minorsky, Reference 5, pages 506-509).

-
1. The spring force on the supported weight is given by:

$$T_2 = ky_2 = \frac{I \cdot kg}{W(v^2 - u^2)} \left\{ \frac{2 \frac{kg}{w} - u^2}{u} \sin ut - \frac{2 \frac{kg}{w} - v^2}{v} \sin vt \right\}$$

If the spring no longer vibrates, kg/w and u vanish, and v^2 becomes kg/W . Thus, the equation reduces to $T_2 = Ia(\cos at)$ as before.

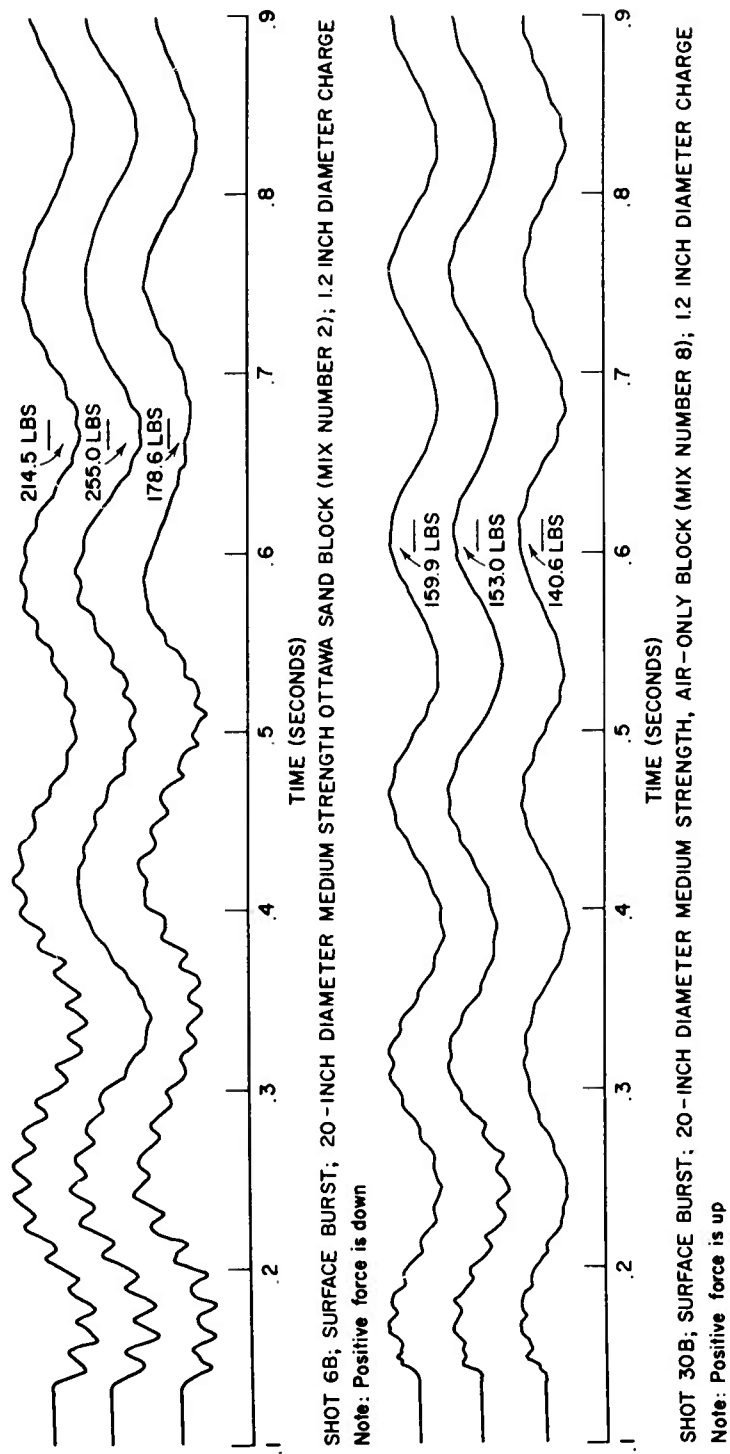


Figure 8

TYPICAL OSCILLOGRAPH RECORDS

Measurements were made of the damping of the lower frequency oscillation with time during the first second after the explosion (6 to 9 cycles). It was found that the attenuation was very small, the amplitude of oscillation decreasing less than 5 percent in that time period. When no viscous damping occurs, integration over any quarter cycle (between a spring force of zero and a maximum force, either positive or negative) will yield the impulse imparted to the system and will yield the same value as an integration performed over the entire record from its start to the time of the same maximum force. Both types of integrations were performed on the first records analyzed, and it was found that the results from quarter-cycle integrations were essentially the same as those from complete record integration. Computations of impulse, therefore, were based on the shorter integrations.

Variations in output from load cell to load cell were somewhat larger than anticipated. The ranges may be seen by reference to the tabulated values in the appendix.

Air impulse measuring system. The air impulse measuring system consisted of three flush-mounted, surface, air pressure gauges spaced from 7 inches to 16.5 inches from the charge with the 16-inch diameter blocks, and from 9 inches to 19.5 inches from the charge with the 20-inch diameter blocks. Thus, the first gauge station for all blocks was located in the blocks themselves.

It was noted in the first part of this report, that the information from the air pressure pulse traces could hopefully be used to determine the equivalent weight of charge which, if exploded in free air, would yield the pressure measured at each station for each shot. The technique used for these determinations was to find from figure 9 at what scaled distance $d/Y^{1/3}$ (distance divided by the cube root of the charge weight) from a charge in free air the recorded pressures would be experienced. By dividing the actual distance to the individual stations by the $d/Y^{1/3}$ value found as above, the cube root of the equivalent free air charge was calculated.

The technique was generally successful, even though surface effects in the immediate vicinity of the charges could

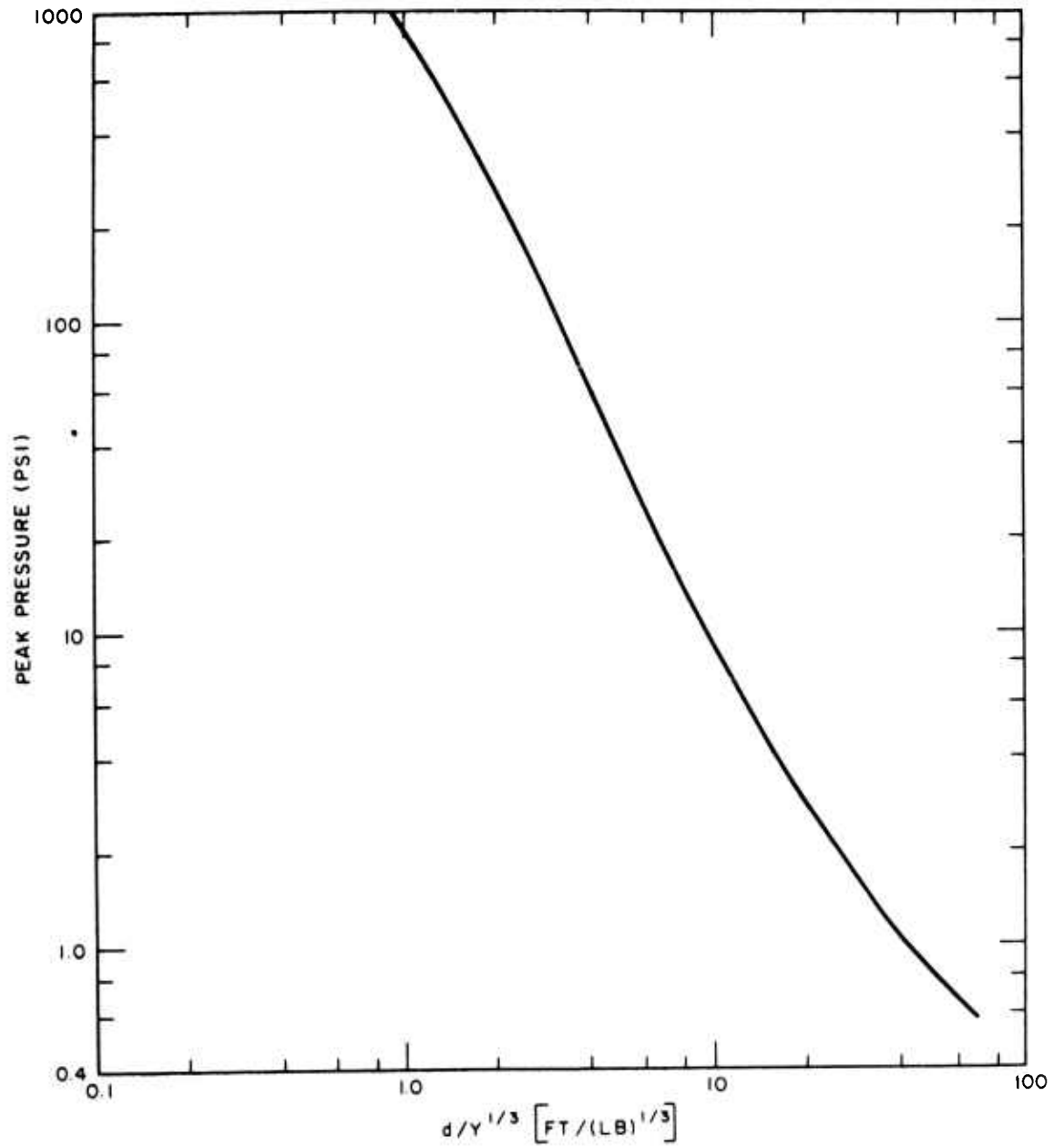


Figure 9

FREE-AIR SHOCK WAVE PEAK PRESSURE VERSUS DISTANCE d
DIVIDED BY CUBE ROOT OF CHARGE WEIGHT Y

Source: Reference 6.

well alter the shock wave from the neat hemispherical shape implied in the calculation. Although in some cases, the calculated effective charge weights for any one shot differed by as much as a factor of two, in many cases calculations from all stations of a particular shot yielded virtually identical effective charge weights.

With the average charge weights thus calculated, estimates of air-shock impulse were made. Reference 6 gives an empirical curve of impulse per unit area as a function of charge weight for distances from the charge as close as 20-charge radii. It was found that data points from that plot at a distance of 20-charge radii from the charge fit quite well a curve from the Kirkwood-Brinkley theory (Reference 7), which could be extended to the charge surface. The two curves were plotted together in figure 10, approximate expressions for each were derived, and integration was performed between the surface of the charge and the edge of the blocks to determine the total impulse (not impulse per unit area) imparted to the blocks by passage of the air shock wave.

This technique most probably does not yield correct results in the immediate vicinity of the crater, but it does afford an approximate method for separating the effect of the impulse imparted to the block by the air shock wave from the total impulse, which includes that directly transmitted from the half buried charge.

Typical records of air shock taken during one shot are shown in Figure 11.

SURFACE BURST GEOMETRY TESTS

Impulse measurements. The results of the impulse measurements are presented in tabular form in tables 6 and 7. It appears that for many of the tests, the impulse due to the air shock wave moving over the block surface (especially for the 16-inch diameter blocks) was nearly constant. This held for the 20-inch diameter blocks as well, except for the values associated with the low strength Ottawa sand and air aggregate mixes.

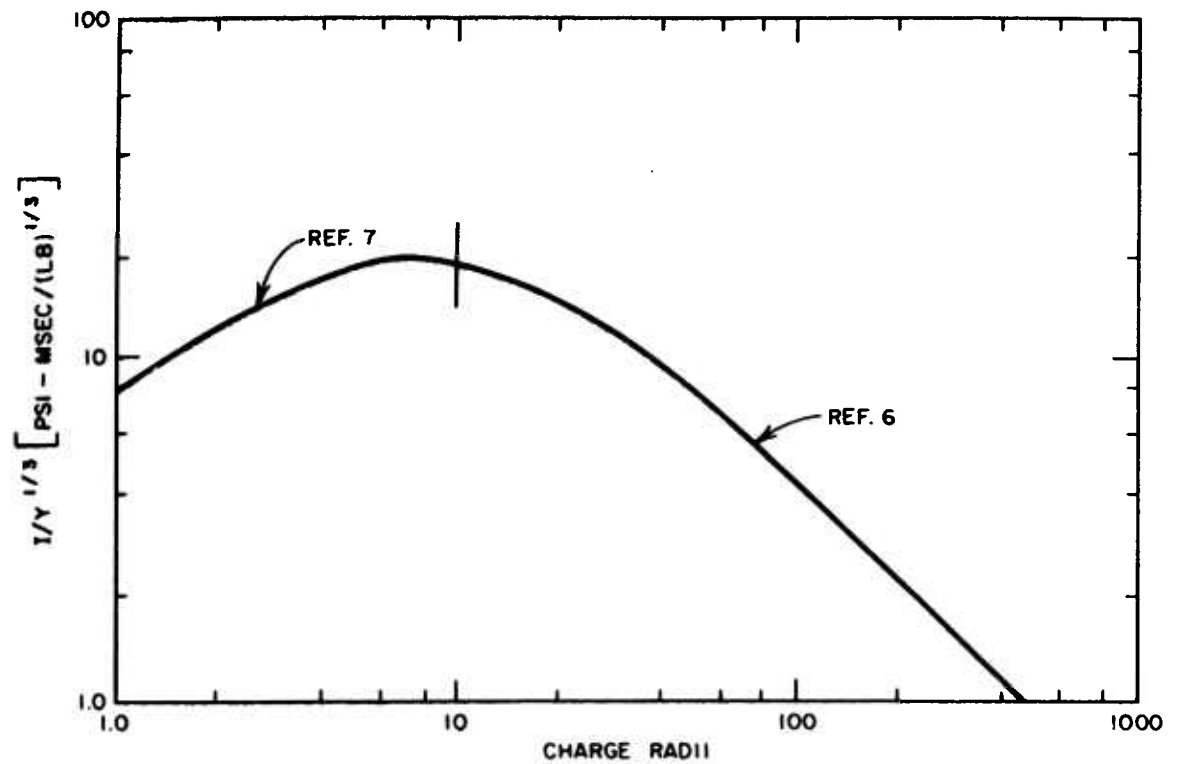


Figure 10

FREE-AIR SHOCK WAVE SIDE-ON IMPULSE PER UNIT AREA I
DIVIDED BY CUBE ROOT OF CHARGE WEIGHT Y VERSUS DISTANCE
IN CHARGE RADII

Sources: References 6 and 7.

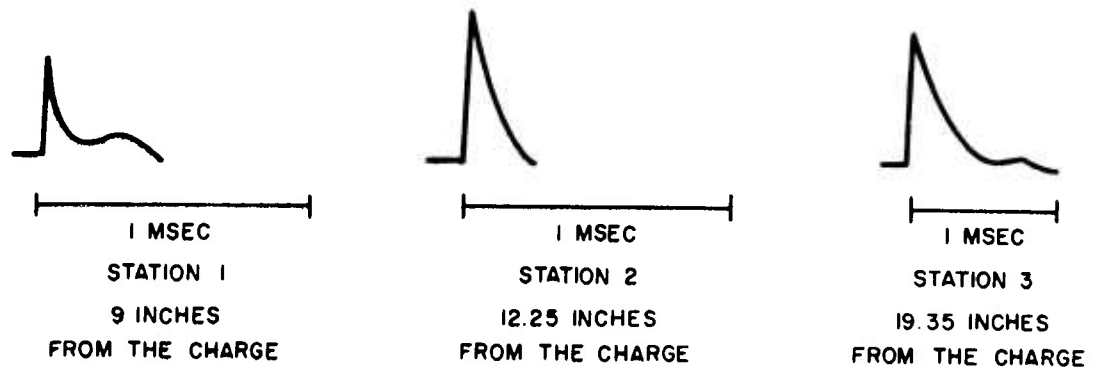


Figure 11

TYPICAL AIR PRESSURE GAUGE TRACES

Note: Shot 6B, surface burst, 20-inch diameter block,
1.2-inch diameter charge.

Table 6

IMPULSE MEASUREMENTS AND CALCULATIONS
 16-Inch Diameter, Surface Geometry Tests, 0.8-Inch Diameter Charge

<u>Shot Number</u>	<u>Total Impulse I_T (lb-sec)</u>	<u>I_T/Y^1 (lb-sec/ lb)</u>	<u>Air Impulse I_A (lb-sec)</u>	<u>$\Delta I = I_T - I_A$ (lb-sec)</u>	<u>$\Delta I/Y$ (lb-sec/ lb)</u>	<u>Y_e^2 (grams)</u>
1A	4.94	316				
B	5.18	323				
5A	4.33	277	0.76	3.57	229	5.1
B	4.61	296	.75	3.86	248	4.8
9A	3.10	199	.75	2.35	150	4.9
B	2.41	155	.68	1.73	111	3.7
13A	3.39	216	.72	2.67	171	4.2
B						
17A	2.96	190	.71	2.25	144	4.2
B	3.22	206	.73	3.49	223	4.5
21A	4.45	285	.67	3.78	242	3.4
B	4.06	260	.74	3.32	212	4.8
25A	2.72	174	.73	1.99	128	4.4
B	3.54	226	.73	1.81	116	4.9
29A	3.00	192	.82	2.18	140	6.4
B			0.72			4.2
33A						
B						

1. $Y = 0.01562$ pounds = charge weight.

2. Y_e = charge weight effective in generating air impulse.

Table 7

IMPULSE MEASUREMENTS AND CALCULATIONS
20-Inch Diameter, Surface Geometry Tests, 1.2-Inch Diameter Charges

<u>Shot Number</u>	<u>Total Impulse I_T (lb-sec)</u>	<u>I_T/Y^1 (lb-sec/ lb)</u>	<u>Air Impulse I_A (lb-sec)</u>	<u>$\Delta I =$ $I_T - I_A$ (lb-sec)</u>	<u>$\Delta I/Y$ (lb-sec/ lb)</u>	<u>Y_e^2 (grams)</u>
2A	19.54	365				
B	17.19	322				
6A	17.46	326	2.01	15.45	288	22.0
B	16.29	306	1.85	14.44	268	20.2
10A	10.04	188	1.67	8.37	156	12.7
B	8.44	158	1.93	6.51	122	19.2
14A			1.81			15.8
B			1.81			16.1
18A	12.62	237	1.77	10.85	203	14.9
B	13.54	253	1.67	11.87	222	14.8
22A	11.17	208	1.82	9.35	175	16.9
B	9.09	170				
26A			1.95			20.4
B	9.89	185	2.00	7.89	147	21.9
30A	9.86	184	1.95	7.91	148	19.9
B	10.84	203	1.99	8.85	165	22.2
34A	9.93	186	1.54	7.39	138	10.0
B	9.57	179	1.47	8.10	152	8.8

1. $Y = 0.0536$ pounds = charge weight.

2. Y_e = charge weight effective in generating air impulse.

Tables 6 and 7 also show the charge weight effective in generating the air impulse, and it is of interest to note the magnitude of the values of effective charge weight relative to actual charge weight. The charge weights shown are those that would generate a spherical rather than a hemispherical shock and, therefore, they should be halved before such a comparison is made. The values do indicate that up to 45 percent of the 1.2-inch diameter (24.3-gram) charges and up to 35 percent of the 0.8-inch diameter (7.1-gram) charges go into generating the air shocks that travel outward over the blocks.

Note in the tables that both the total impulse and the directly transmitted impulse (total less that from air shock) are divided by the actual charge weight. According to ordinary charge weight scaling, the total impulse delivered by two charges of different weights should be proportional to the charge weights, and, therefore, in otherwise identical experiments, the ratio of impulse to charge weight should remain constant.

In figure 12, both total impulse and the ratio of total impulse to charge weight are plotted for all surface bursts for which data are available as a function of Young's modulus. With the exception of the points for the weakest pumice mix, ordinary cube root scaling appears to hold since the plotted ratios from the tests with 0.8-inch diameter charges lie very close to those from tests with 1.2-inch diameter charges.

Figure 12 also shows a strong relationship between scaled impulse and Young's modulus. Most of the materials tested had Young's moduli of less than 2×10^6 psi, but two of the mixes containing Ottawa sand had Young's moduli of greater than 4×10^6 . Tests with these two mixes resulted in the largest impulses recorded. Young's modulus is related to the compressibility of a sample; thus, with all materials except the weakest pumice mix, there is strong indication that impulse transmitted to a material is a function of its compressibility.¹

-
1. A similar relationship holds between impulse and the calculated shear and bulk moduli. These, however, are derived from Young's modulus and Poisson's ratio (which was nearly constant).

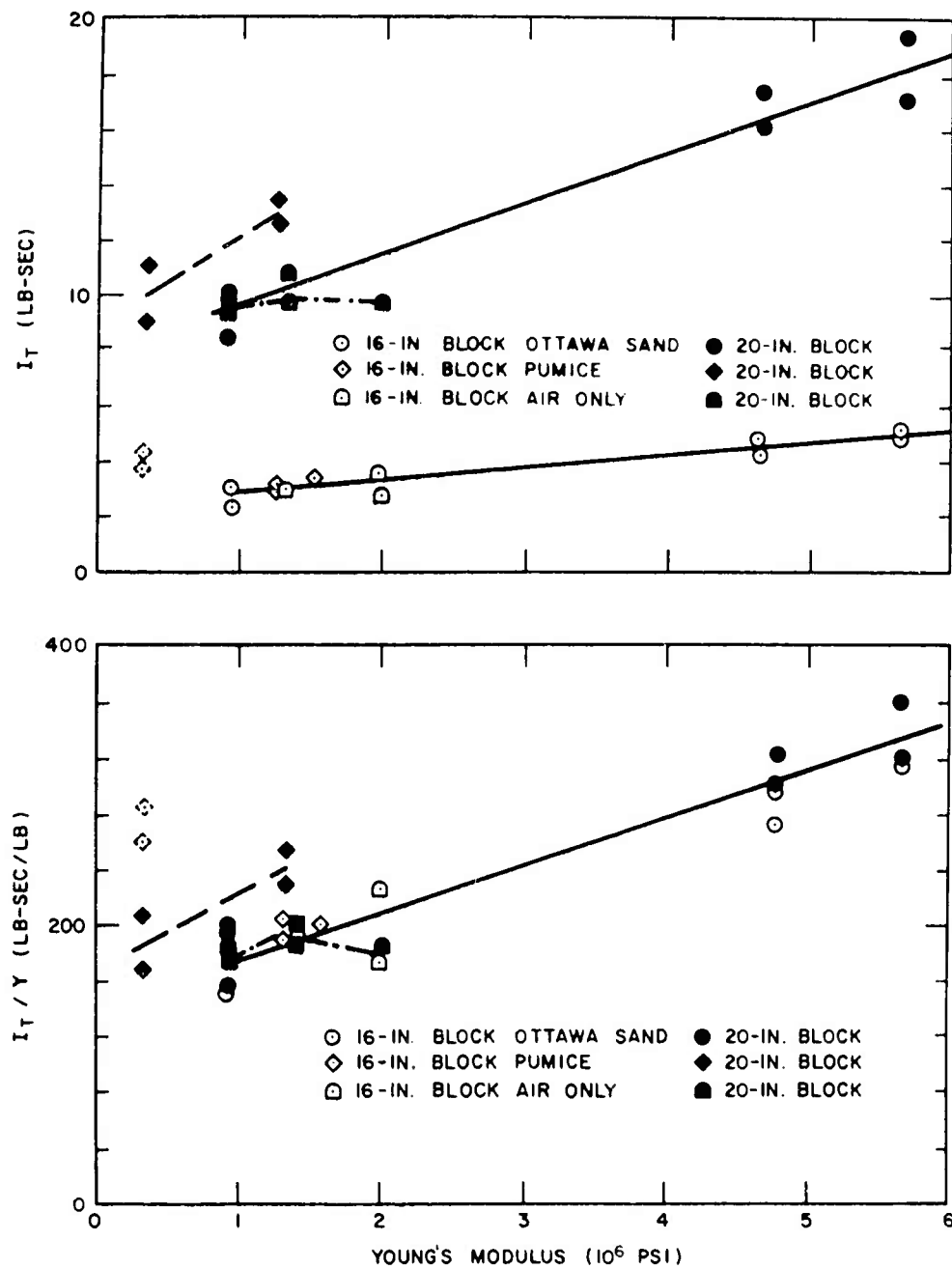


Figure 12

IMPULSE I_T AND IMPULSE I_T DIVIDED BY CHARGE WEIGHT Y
VERSUS YOUNG'S MODULUS

Other less striking relationships between impulse and material properties also hold. Thus, transmitted impulse appears to increase with increase in compressive strength, shear strength, and bulk density, as well as in Young's modulus.

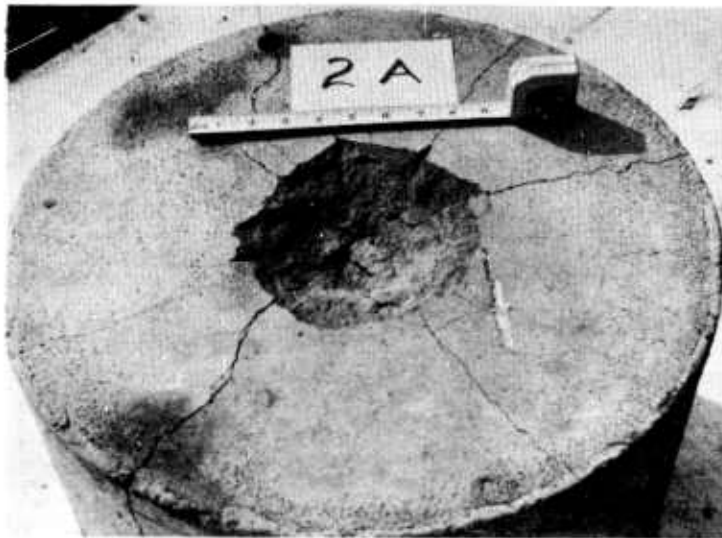
Energy measurements. Calculations were made of the potential energy of the spring mass system stored at its maximum deflection which, in an undamped system, is equal to the kinetic energy imparted to the system by an impulsive force. This quantity is of limited interest, since, for a given impulse, its value depends entirely on the period or frequency of the system; as the period of a system increases, the potential energy stored at maximum deflection decreases.

For the 16-inch blocks, the energy calculated as indicated above ranged between 20 and 60 in-lb and for the 20-inch blocks, between 100 and 400 in-lb. This compares with approximately 3×10^5 in-lb of explosion energy yielded by the 0.8-inch diameter charges, and approximately 1×10^6 in-lb of explosion energy yielded by the 1.2-inch diameter charges.

Crater measurements. Crater dimensions were difficult to obtain in certain cases. Some craters were quite regular, resembling paraboloids, others were stepped, with deep, central, generally spherical holes surrounded by annuli of smaller depths. The differences in crater shapes obtained are illustrated in figures 13 and 14 which show views of the craters from above, in 20-inch diameter blocks of the high compressive strength mixes with each aggregate (Ottawa sand, pumice, and air only) along with a sectioned view of the crater in one of the 16-inch diameter blocks of the low compressive strength material containing pumice.

Crater measurements that were made are tabulated in tables 8 and 9. The entries under "diameter" represent approximate diameters of the central crater, and of shallower steps if any could be discerned.

Although the irregular nature of many of the craters precludes accurate determination of scaling relationships, it appears that cube root scaling applies. The measurement of



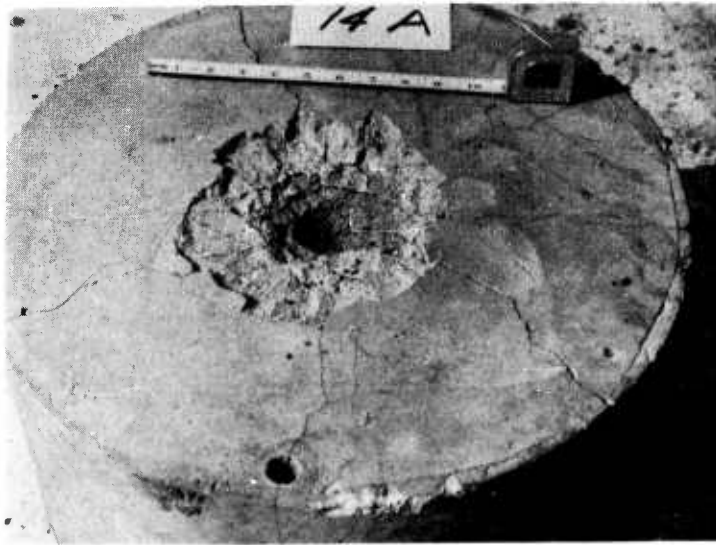
A. Ottawa Sand Aggregate



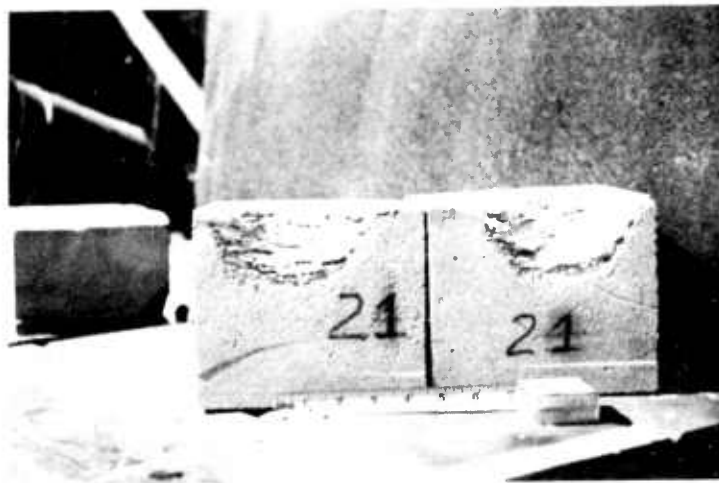
B. Air Aggregate

Figure 13

CRATERS FROM SURFACE BURSTS IN HIGH COMPRESSIVE STRENGTH
20-INCH DIAMETER BLOCKS



A. High Compressive Strength, 20-inch Diameter Block



B. Low Compressive Strength, 16-inch Diameter Block

Figure 14

CRATERS FROM SURFACE BURSTS IN HIGH COMPRESSIVE STRENGTH AND
LOW COMPRESSIVE STRENGTH BLOCKS OF MIXES CONTAINING PUMICE
AGGREGATE

Table 8

CRATER MEASUREMENTS
 16-Inch Diameter, Surface Geometry Tests,
 0.8-Inch Diameter Charges

<u>Shot Number</u>	<u>Depth (inches)</u>	<u>Diameter (inches)</u>		<u>Volume (cubic inches)</u>
		<u>Main Crater</u>	<u>Outer</u>	
1A	0.8		4.3	6.2
1B	0.8		4.3	
5A	0.9		4.5	6.0
5B	1.0		4.6	7.7
9A	1.3	1.8	4.6	8.4
9B	1.3	1.9	4.8	7.5
13A	1.1	1.5	3.0	4.9
13B				
17A	1.1	1.6	6.3	10.2
17B	1.3	1.6	6.3	7.0
21A	1.9		4.6	22.8
21B	1.9		4.5	21.6
25A	1.1	1.8	5.5	5.0
25B	1.1	1.6	4.5	4.9
29A	1.1	2.1	3.5	4.2
29B	1.1	1.6	4.5	6.7
33A	1.1	2.0	3.5	7.0
33B	1.3	2.0	3.5	

Table 9

CRATER MEASUREMENTS
20-Inch Diameter, Surface Geometry Tests,
1.2-Inch Diameter Charges

<u>Shot Number</u>	<u>Depth (inches)</u>	<u>Diameter (inches)</u>			<u>Volume (cubic inches)</u>
		<u>Main Crater</u>	<u>Step</u>	<u>Outer</u>	
2A	1.4			7.0	23.6
2B	1.4			6.1	20.1
6A	1.8			7.5	38.3
6B	1.4			7.0	
10A	2.1	2.5	4.1	6.3	29.9
10B	2.3	2.0	4.0	6.3	
14A	1.8	2.5		7.0	28.4
14B	1.6	2.6		7.0	
18A	1.8	2.3		8.5	48.7
18B	1.8	2.3		7.3	
22A	3.3			7.5	83.1
22B	3.0			7.0	
26A	1.5	2.3		7.5	22.0
26B	1.6	2.5		6.0	
30A	1.6	2.8		6.3	21.2
30B	1.5	2.8		6.5	
34A	1.8	2.4		6.0	25.5
34B	1.8	3.0		5.5	

depth is the most sure of those tabulated, and the crater depths from the 1.2-inch diameter charges are approximately 1.5 times as large as those from the 0.8-inch diameter charges. Also, the measured crater volumes from the 1.2-inch diameter charges are about 3.5 times as large as those from the 0.8-inch diameter charges.

One startling, and as yet not fully explained, occurrence was the generation of very much larger craters in blocks made with two of the pumice mixes than in any other block. The volume of the largest crater was more than twice as large as that of any other crater.

On the assumption that crater formation is related primarily to shear strength and local crushing strength (of which bulk density should be a measure), figure 15 was prepared in which crater volume is plotted against the inverse of the product of bulk density and internal shear strength. There appears to be some correlation in that crater volumes in all material (including one of the pumice mixes) for which the inverse of the product ranges between 0 and 3×10^5 are between 20 and 40 inches³, and as the ratio increases, the crater volume does too.

SPLIT-SAMPLE GEOMETRY TESTS

It has already been noted that no data could be acquired from the 20-inch diameter split-sample tests when the 0.8-inch diameter charges were employed. In the final tests with this geometry, the firing with 0.6-inch diameter charges was accomplished with each block in a steel sleeve except in one case; during that test, the lower block broke.

Only information from the spring mounting system and high-speed motion pictures were taken during this series. Unfortunately, the ratio of successful to unsuccessful firings was lower during this series than during any other. Table 10 gives impulse and crater data, and figure 16 shows a series of frames from the motion picture record of one of the tests.

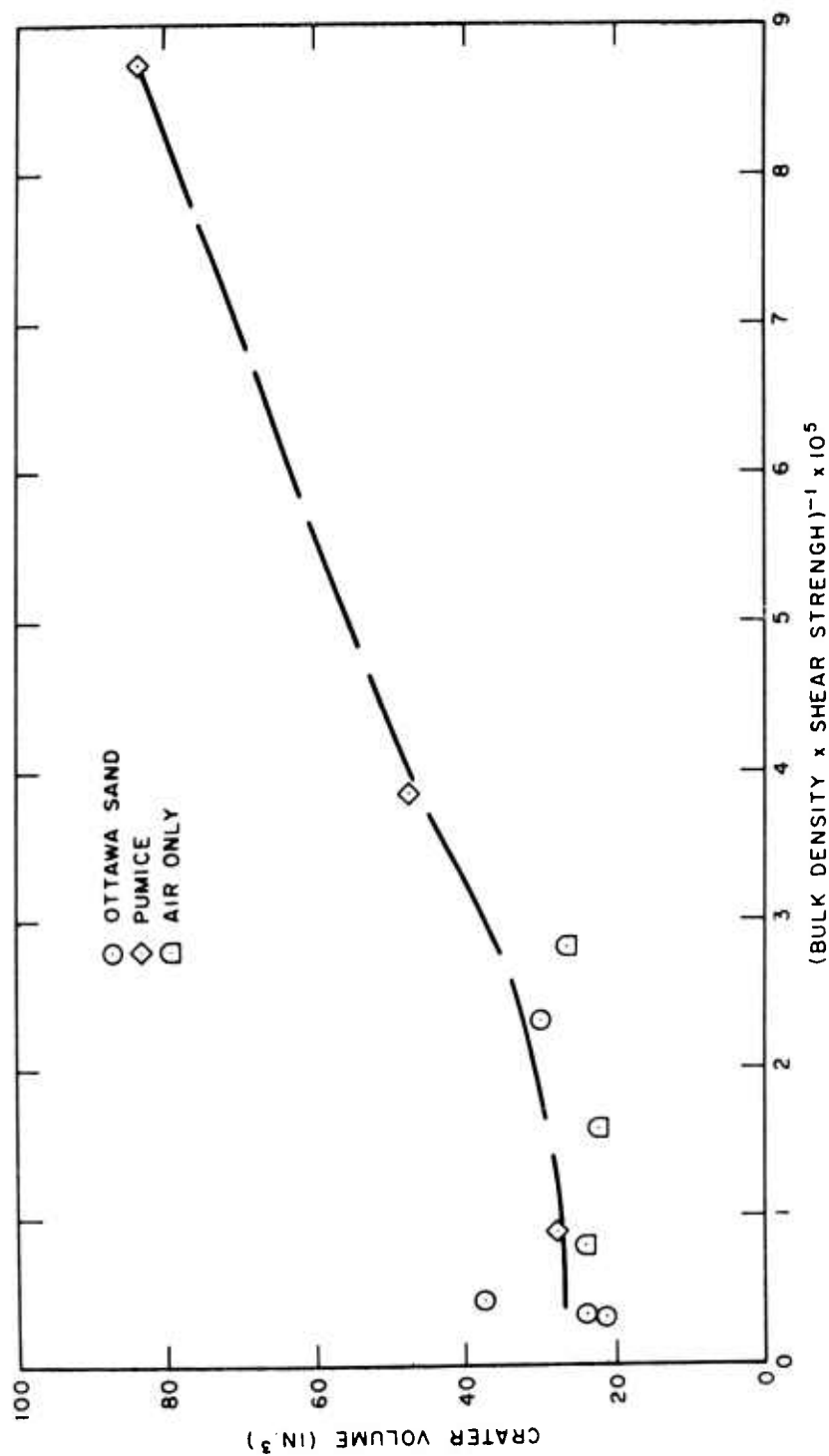


Figure 15

CRATER VOLUMES FROM SURFACE BURSTS ON 20-INCH DIAMETER BLOCKS VERSUS THE INVERSE OF THE PRODUCT OF BULK DENSITY AND INTERNAL SHEAR STRENGTH

Note: Bulk density and shear strength units are as given in table 5.

Table 10

IMPULSE AND CRATER MEASUREMENTS
20-Inch Diameter, Split-Sample Geometry Tests,
0.6-Inch Diameter Charges

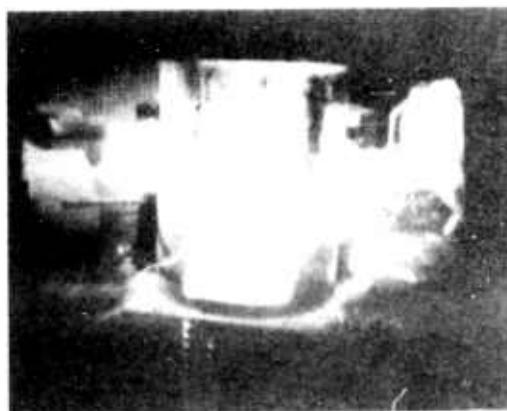
Shot Number	Impulse (lb-sec)	Depth (inches)	Diameter (inches)		Volume (cubic inches)	Remarks
			Main Crater	Outer		
4A'	43.7				1.2	
4B'	40.6	0.6		1.3	1.0	
8A'	40.0	0.6		1.1		
12A'	24.6				1.6	Charge misfire
12B'						
16A'	14.6					Blocks not keyed
16B'						Blocks not keyed
20A'	28.0	0.9	1.6	2.8	1.3	
20B'						Charge misfire
24A'	16.4	1.1		2.4	3.3	
28A'	33.7	0.8		1.3	0.6	Block split
28B'	32.6	0.6	2.1	3.0	1.5	
32A'						Blocks not keyed
32B'						Blocks not keyed
36A'						Blocks not keyed
36B'						Blocks not keyed



A. Before detonation



B. First visible movement



C. ~16 msec after B



D. ~100 msec after B

Figure 16

FRAMES FROM MOTION PICTURE RECORD OF A SPLIT-SAMPLE
GEOMETRY TEST

Note: Block 8A', Mix 2, 0.8-inch diameter charge.

Impulse measurements. As was expected, the impulses recorded from shots in this geometry were far greater than those from surface bursts, even though the charge used was the smallest successfully employed. Impulses from these tests with 0.6-inch diameter charges were generally two to three times as large as those from surface burst geometry tests with the 1.2-inch diameter charges, though the explosive energy was only one-eighth as great. It is clear from this that the effective loading duration must have been lengthened considerably, since impulse is $\int F dt$, and the initial forces should scale as the charge weight.

Since impulse has been shown to be directly proportional to the charge weight, it can be inferred that impulses from the split-sample geometry should be roughly the same as those from the 1.2-inch diameter charges in the surface burst configuration if the charge size were reduced to between 0.4 and 0.5 inch in diameter.

It cannot be determined from these tests what portion of the impulse that drove the blocks downward was applied outside the immediate crater area. There was clear indication that the fit of the two blocks of the split sample was quite critical in determining the impulse.

Crater measurements. The craters that formed in the split-sample geometry were far different from those that formed in the surface burst geometry. They were much more nearly paraboloidal in shape, with the ratio between crater diameter and depth being generally much smaller than that observed from surface bursts. However, where a clearly identifiable central hole appeared in the surface shots, its diameter-depth ratio was approximately the same as that in the split-sample shots.

Two views of the craters formed in two tests are shown in figures 17 and 18. Note the general regularity of shape in the sectioned samples.

Crater depths were approximately two-thirds those of the surface burst geometry tests with the 0.8-inch diameter charges. From this, cube root scaling indicates that crater depths from 0.8-inch diameter charges in the split-sample geometry would

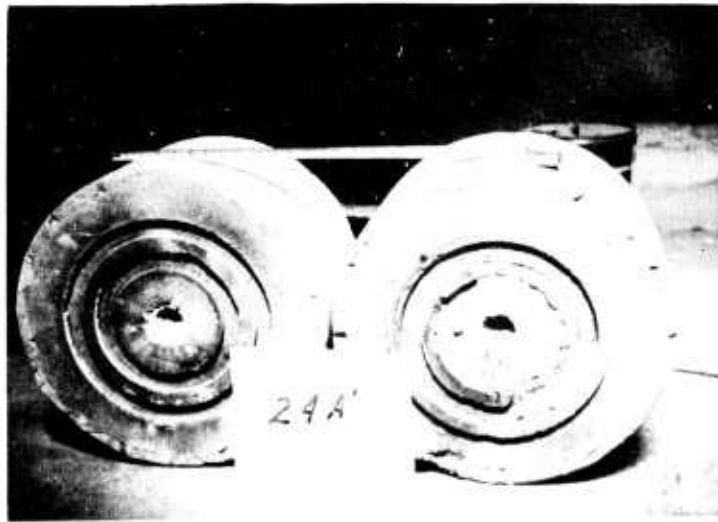


Figure 17

CRATERS IN SPLIT-SAMPLE GEOMETRY BLOCKS

Note: Sample 24A', Mix 6, 0.6-inch diameter charge.

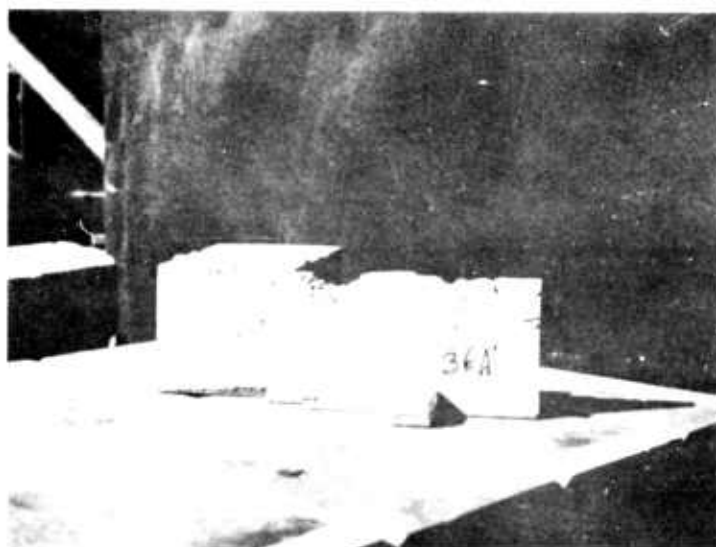
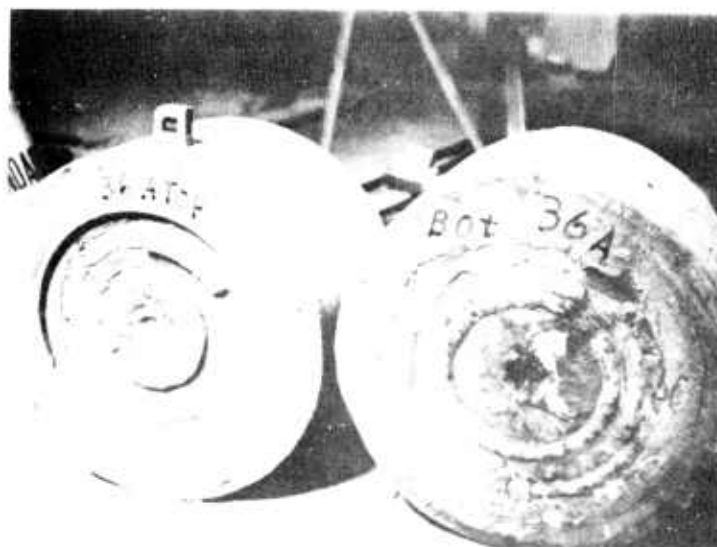


Figure 18

CRATERS IN SPLIT-SAMPLE GEOMETRY BLOCKS

Notes: Sample 36A', Mix 9, 0.6-inch diameter charge.
Sectioned view shows edges and center of crater.

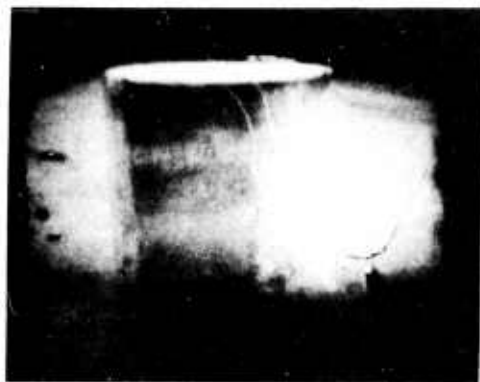
have been approximately the same as those observed with this size of charge in surface bursts. This conclusion is partly borne out by the observation that in many of the surface bursts, a regular, central crater formed about the charge, probably before stress relief due to the presence of a free upper surface could make itself felt. If that is the case, then the central craters (in the split-sample geometry, the main craters) would be formed in the same way for both surface and split-sample geometry tests.

TOTALLY CONTAINED GEOMETRY TESTS

The first tests conducted during the formal explosion test program were shots 37, 38, and 39, the tests using high strength mixes of each aggregate in totally contained geometries (i.e. with the charges integrally cast). It was inferred from preliminary tests with 20-inch diameter split-sample geometry blocks that this diameter would be adequate for use with 0.8-inch diameter charges. This was not correct. All blocks shattered. Frames from a film record of one of the tests are shown in figure 19.

At the very end of the program, the tests were repeated using 0.6-inch diameter charges. These tests were far more successful and revealing than those of the first series had been, even though many blocks did break. The two containing Ottawa sand as an aggregate each broke into only two pieces through the charge position and approximately along a plane normal to the axis of the blocks. (When the blocks were cast, the charges had been supported by a wire normal to the block axis at about mid height, and in each case, the break was along this wire.) This type of breakage permitted measurements to be made of the dimensions of the cavities formed around the charge position, but cavity volumes could not be measured because the break was not truly plane. The cavities appeared to be spherical, although measurements indicated that horizontal cavity dimensions were somewhat larger than the vertical dimensions.

One of the blocks containing pumice as an aggregate broke into three pieces, with the major break being along a diagonal



A. At detonation
(Note sparking,
lower right.)



B. ~1 msec after detonation



C. ~6 msec after
detonation



D. ~15 msec after detonation

Figure 19

FRAMES FROM MOTION PICTURE RECORD OF FIRST TOTALLY CONTAINED
GEOMETRY TESTS

Note: Block 37A, Mix 1 (high strength, Ottawa sand),
0.8-inch diameter charge.

plane through the charge position from the top to the bottom of the block. All previous breaks had been normal to the axis of the blocks and could have been caused by a plane of weakness between the two batches of material that made up the blocks. The break in the block containing pumice was clearly not related to this cause. Again, measurements of cavity dimensions were readily made.

The second block containing pumice did not break, although a high-speed motion picture record clearly showed that the charge detonated. (The block increased slightly in diameter, and remained in this bulged condition.) Because of the possibility of the existence of high internal pressures, the block was not opened to its internal cavity until a week after the test. When it was so opened, a highly spherical cavity 1.75 inches in diameter was found.

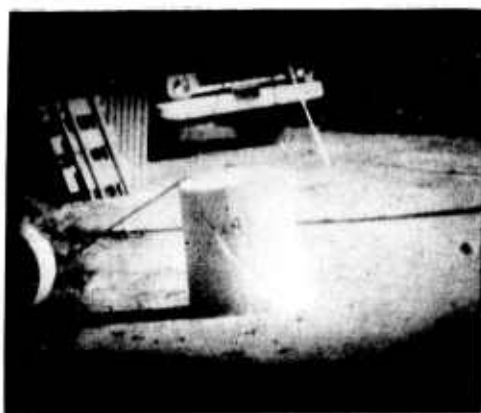
Of the two blocks containing the air aggregate, only one could be used, the second having broken sometime during the curing cycle. The one that was used ruptured, but the failure was clearly borderline; after the test, the block was still in place though in a number of pieces. Unfortunately this type of breakage did not permit measurement of cavity dimensions. Cavity dimensions recorded during the test are shown in table 11.

Table 11

CAVITY DIMENSIONS				
TOTALLY CONTAINED GEOMETRY				
0.6-Inch Diameter Charge				
<u>Shot No.</u>	<u>Mix No.</u>	<u>Cavity Depth (inches)</u>	<u>Cavity Diameter (inches)</u>	<u>Remarks</u>
37A'	1	0.5	1.38	Circular hole
37B'	1	0.4	1.38	Circular hole
38A'	4	0.8	1.38 - 1.75	Elliptical hole
38B'	4	-	1.75	Spherical cavity

Frames from the high-speed motion picture record of shot 38A' are shown in figure 20.

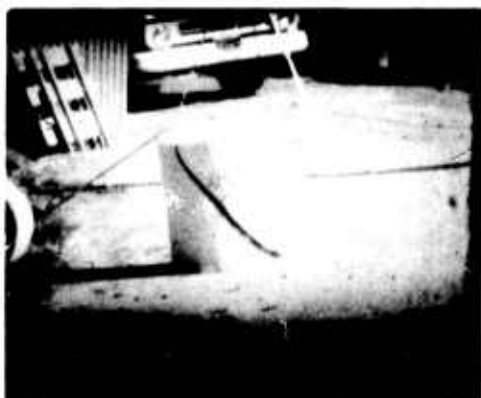
The crater dimensions shown in table 10 for the split-sample geometry tests with the high strength Ottawa sand mix are very close to the cavity dimensions shown in the first two entries in table 11 for totally contained geometry tests of the same material. From this, it can be inferred that split-sample geometries are good simulants of totally contained geometries, at least for generating craters.



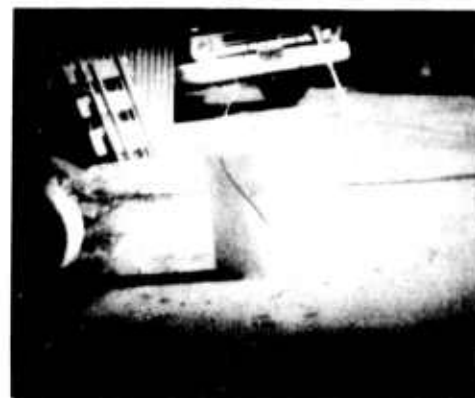
A. Before detonation



B. First visible movement



C. ~5 msec after B



D. ~15 msec after B

Figure 20

FRAMES FROM MOTION PICTURE RECORD OF SECOND TOTALLY CONTAINED
GEOMETRY TEST

Note: Block 38A', Mix 4, 0.6-inch diameter charge.

Section IV

CONCLUSIONS

Results of tests conducted during this program indicate that material properties have a major effect on the impulse transmitted to rock-like materials by explosive energy releases and on the formation of craters within these materials. Thus, impulse, in a sense a measure of the efficiency of transmission of explosion energy to the materials, varied by as much as a factor of two for the materials tested. The compressibility (as measured by Young's moduli) of the materials was perhaps the most important property affecting impulse transmission.

Estimates made of the impulse transmitted to the sample rock-like materials by the air shock waves that travel out from a surface burst indicate that this quantity is but little affected by the properties of the material on which the burst takes place. It was also found that approximately 30 or 40 percent of explosion energy from a surface burst is used to create the air shock wave.

Material properties were found to have a very large influence on the sizes and shapes of craters formed by explosions. Crater volumes, for example, in one material were more than twice as large as volumes in other materials. The most important material properties affecting crater formation appeared to be those of internal shear strength and those reflecting the internal cellular structure of the materials, as measured by their bulk densities. The one material that displayed the widest variation in this combination of properties also displayed by far the widest variation in the volumes of craters produced by an explosion.

Although some crater dimensions were difficult to measure, they appeared to scale approximately as the cube root of the charge size (or explosive energy release).

A tentative conclusion arrived at was that crater formation mechanisms directly beneath a charge in a surface burst probably resemble those around a totally contained charge.

Scaled crater depths (crater depth divided by the cube root of the charge weight) in surface burst geometries, in geometries in which the burst takes place at the interface between two blocks, and in geometries in which the burst is totally contained, were approximately the same.

LIST OF REFERENCES

1. 1961 Book of ASTM Standards, Part 4. Philadelphia: American Society for Testing and Materials, 1961.
2. Taylor, D. W. Fundamentals of Soil Mechanics. New York: John Wiley and Sons, Inc., 1948.
3. Rinehart, J. W. "More Experiments Pertaining to the Design of Underground Openings Subjected to Intense Ground Shocks," Shock, Vibration and Associated Environments, Bulletin No. 29, Part III, pp 169-187, July, 1961.
4. Timoshenko, S. Vibration Problems in Engineering. New York: D. Van Nostrand Co., Inc., 1953.
5. Minorsky, N. Nonlinear Oscillations. Princeton: D. Van Nostrand Co. Inc., 1962.
6. Goodman, H. J. Compiled Free-Air Blast Data on Bare Spherical Pentolite, BRL Report 1092. Aberdeen Proving Ground: Ballistic Research Laboratories, 1960.
7. Dewey, J. and Sporrazza, J. The Effect of Atmospheric Pressure and Temperature on Air Shock, BRL Report 721. Aberdeen Proving Ground: Ballistic Research Laboratories, 1950.

Appendix

TABULATED LOAD CELL
AND
AIR PRESSURE GAUGE DATA

Table 12

LOAD CELL AND AIR PRESSURE GAUGE DATA

Shot Number	Maximum Force T_m (lb) and Impulse I_T (lb-sec)						Peak Pressure (psi) ¹		
	Load Cell 1		Load Cell 2		Load Cell 3		Station 1	Station 2	Station 3
	T_m	I_T	T_m	I_T	T_m	I_T			
1A	93.6	1.46	102.0	1.88	79.8	1.60			
1B	101.4	2.12	97.8	1.59	79.8	1.47			
2A	249.6	6.23	318.6	7.66	209.0	5.65			
2B	241.8	6.10	280.5	7.08	152.0	4.01			
4A'	518.0	12.27	672.0	17.14	540.0	14.28			
4B'	564.3	12.89	732.0	14.28	636.0	13.46			
5A	70.2	1.33	85.0	1.45	68.4	1.55	127	85.6	21.4
5B	74.1	1.46	85.0	1.73	68.4	1.42	117	81.5	21.0
6A	210.6	5.70	255.6	7.37	152.0	4.39	146	146.0	42.0
6B	214.5	5.57	255.0	6.07	178.6	4.65	152	137.0	37.8
8A'	499.5	12.27	600.0	14.28	576.0	13.46			
8B'									
9A	54.6	0.93	38.3	1.01	41.8	1.16		56.5	18.5
9B	50.7	0.93	46.8	0.58	45.6	0.90	93.3	53.7	23.3
10A	167.7	3.05	174.3	3.76	136.8	3.23	173	85.0	
10B	144.3	3.18			114.0	2.45	250	106.0	

Table 12 Continued

Shot Number	Maximum Force T_m (lb) and Impulse I_T (lb-sec)						Peak Pressure (psi) ¹		
	Load Cell 1		Load Cell 2		Load Cell 3		Station 1	Station 2	Station 3
	T_m	I_T	T_m	I_T	T_m	I_T			
12A' 12B'	296.0	7.86	360.0	8.98	312.0	7.75			
13A 13B	54.6	1.06	63.8	1.30	49.4	1.03			19.5
14A 14B							182 193	111 116	35.8
16A' 16B'	222.0	4.40	264.0	5.71	204.0	4.49			
17A 17B	62.4 66.3	0.93 1.06	63.8 59.5	0.87 0.87	38.0 45.6	1.16 1.29	121 156	65.2 61.5	26.2 18.7
18A 18B		4.64		4.62		3.36	158 180	84.5 101	29.8 35.6
20A' 20B'	351.5	7.23	456.0	11.42	384.0	9.38			
21A 21B	76.0 64.0	1.77 1.35	60.2 64.5	0.91 1.16	78.0 65.0	1.77 1.54	100 169	63.9 61.5	16.7 19.7
22A 22B	171.0 132.0	3.94 2.99	136.0 137.6	3.51 3.07			164	132	34.3

Table 12 Continued

Shot Number	Maximum Force T_m (lb) and Impulse I_T (lb-sec)						Peak Pressure (psi) ¹		
	Load Cell 1		Load Cell 2		Load Cell 3		Station 1	Station 2	Station 3
	T_m	I_T	T_m	I_T	T_m	I_T			
24A'	222.0	5.03	264.0	6.52	240.0	4.90			
24B'									
25A	66.3	0.93	68.0	1.01	57.0	0.78	138	71.5	20.7
25B	62.4	1.06	68.0	1.45	57.0	1.03	120	79.7	20.6
26A							181	125	38.2
26B	195.0	3.71	212.5	3.47	133.0	2.71	209	130	41.7
28A'	490.3	10.06	624.0	14.28	552.0	9.38			
28B'	416.3	9.75	504.0	12.65	432.0	10.20			
29A	58.5	0.80	55.3	1.17	53.2	1.03			25.7
29B							129	71	20.8
30A	144.3	3.45	157.3	3.18	152.0	3.23	220	129	
30B	159.9	3.71	153.0	3.90	140.6	3.23	209	135	44.6
32A'									
32B'									
33A									
33B									

Table 12 Continued

Shot Number	Maximum Force T_m (lb) and Impulse I_T (lb-sec)				Peak Pressure (psi) ¹		
	Load Cell 1		Load Cell 2		Station 1	Station 2	Station 3
	T_m	I_T	T_m	I_T			
34A	148.0	3.26	120.4	3.36	214	147	25.4
34B	148.0	3.67	116.1	2.78	188	143	33.4
36A'							
36B'							

1. No pressure measurements made on shots 4, 8, 12, 16, 20, 24, 28, 32, and 36 (split sample).

Distance to charge for shots 1, 5, 9, 13, 17, 21, 25, 29, and 33 (16-inch diameter block) Station 1 = 7 inches, Station 2 = 9.5 inches, Station 3 = 16.5 inches.

Distance to charge for shots 2, 6, 10, 14, 18, 22, 26, 30, and 24 (20-inch diameter block) Station 1 = 9 inches, Station 2 = 12.3 inches, Station 3 = 19.3 inches.

DISTRIBUTION

No. Cys

HEADQUARTERS USAF

1	Hq USAF (AFOCE), Wash 25, DC
1	Hq USAF (AFRST), Wash 25, DC
1	Hq USAF (AFRNE-A, Maj Lowry), Wash 25, DC
1	Hq USAF (AFTAC), Wash 25, DC
1	USAF Dep, The Inspector General (AFIDI), Norton AFB, Calif
1	USAF Directorate of Nuclear Safety (AFINS), Kirtland AFB, NM
1	AFOAR, Bldg T-D, Wash 25, DC
1	AFCRL, Hanscom Fld, Bedford, Mass
2	AFOSR, Bldg T-D, Wash 25, DC

MAJOR AIR COMMANDS

1	AFSC, (SCT), Andrews AFB, Wash 25, DC
2	SAC, (OAWS), Offutt AFB, Nebr
1	ADC (Ops Anlys), Ent AFB, Colorado Springs, Colo
2	AUL, Maxwell AFB, Ala
2	USAFIT (USAF Institute of Technology), Wright-Patterson AFB, Ohio
1	USAFE (Dir of Air Targets), APO 633, New York, NY
2	USAFA, United States Air Force Academy, Colo

AFSC ORGANIZATIONS

1	AFSC Regional Office (Maj Blilie), 6331 Hollywood Blvd., Los Angeles 28, Calif
1	FTD (Library), Wright-Patterson AFB, Ohio
2	ASD (ASAPRL), Wright-Patterson AFB, Ohio
1	RTD (Maj Munyon), Bolling AFB, Wash 25, DC
	BSD, Norton AFB, Calif
1	(BST)
1	(BSQ)
1	(BSR)

DISTRIBUTION (Cont'd)

No. Cys

1	ESD (ESAT), Hanscom Field, Bedford, Mass
1	AF Msl Dev Cen (RRRT), Holloman AFB, NM
1	AFFTC (FTFT), Edwards AFB, Calif
1	AFMTC (MTBAT), Patrick AFB, Fla
1	APGC (PGAPI), Eglin AFB, Fla
2	RADC (Document Library), Griffiss AFB, NY
2	AEDC (AEOI), Arnold Air Force Station, Tenn

KIRTLAND AFB ORGANIZATIONS

1	AFSWC (SWEH), Kirtland AFB, NM
	AFWL, Kirtland AFB, NM
25	(WLL)
5	(WLRS)
1	US Naval Weapons Evaluation Facility (NWEF) (Code 404), Kirtland AFB, NM

OTHER AIR FORCE AGENCIES

2	Lowry Tech Tng Cen (Dept of Wpns Tng), Lowry AFB, Colo
	Director, USAF Project RAND, via: Air Force Liaison Office, The RAND Corporation, 1700 Main Street, Santa Monica, Calif
1	(RAND Physics Div)
2	(RAND Library)
1	3415th Technical Training Center (ATC), Lowry AFB, Colo (Nuclear Weapons Branch)

ARMY ACTIVITIES

1	Chief of Research and Development, Department of the Army (Special Weapons and Air Defense Division), Wash 25, DC
1	Redstone Scientific Information Center, US Army Missile Command (Tech Library), Redstone Arsenal, Ala
2	Director, Ballistic Research Laboratories (Library), Aberdeen Proving Ground, Md

DISTRIBUTION (Cont'd)

No. Cys

- 1 Commanding Officer, US Army Signal Research & Development Laboratory, (SIGRA/SL-SAT-1, Weapons Effects Section), Fort Monmouth, NJ
- 1 Research Analysis Corp., (Document Control Office), 6935 Arlington Road, Bethesda, Md., Wash 14, DC
- 1 Hq US Army Air Defense Command (ADGCB), Ent AFB, Colo
- 2 Chief of Engineers, Department of the Army (ENGMC-EM), Wash 25, DC
- 2 Director, US Army Waterways Experiment Sta (WESRL), P.O. Box 60, Vicksburg, Miss
- 2 Commanding Officer, US Army Engineers, Research & Development Laboratories, Ft Belvoir, Va
- 1 Commanding General, White Sands Missile Range (Technical Library), White Sands, NM

NAVY ACTIVITIES

- 1 Chief of Naval Research, Department of the Navy, Wash 25, DC
- 2 Chief, Bureau of Yards and Docks, Department of the Navy, Wash 25, DC
- 1 Commanding Officer, Naval Research Laboratory, Wash 25, DC
- 1 Commanding Officer and Director, David Taylor Model Basin, Wash 7, DC
- 2 Commanding Officer and Director, Naval Civil Engineering Laboratory, Port Hueneme, Calif
- 1 Commander, Naval Ordnance Laboratory, White Oak, Silver Spring, Md
- 1 Officer-in-Charge, Civil Engineering Corps Officers, US Naval School, Naval Construction Battalion Center, Port Hueneme, Calif
- 2 Office of Naval Research, Wash 25, DC

OTHER DOD ACTIVITIES

- 2 Chief, Defense Atomic Support Agency (Document Library), Wash 25, DC
- 1 Commander, Field Command, Defense Atomic Support Agency (FCAG3, Special Weapons Publication Distribution), Sandia Base, NM
- 1 Director, Advanced Research Projects Agency, Department of Defense, The Pentagon, Wash 25, DC

DISTRIBUTION (Cont'd)

No. Cys

- 1 Director, Defense Research & Engineering, The Pentagon, Wash 25, DC
- 1 US Documents Officer, Office of the US National Military Representative (SHAPE), APO 55, New York, NY
- 20 Hq Defense Documentation Center for Scientific and Technical Information (DDC) Arlington Hall Sta, Arlington 12, Va

AEC ACTIVITIES

- 1 US Atomic Energy Commission, Headquarters Library, Reports Section, Wash 25, DC (Mail Station G-017)
- 1 Sandia Corporation (Technical Library), Sandia Base, NM
- 1 Sandia Corporation (Technical Library), P.O. Box 969, Livermore, Calif
- 1 Chief, Division of Technical Information Extension, US Atomic Energy Commission, Box 62, Oak Ridge, Tenn
- 1 University of California Lawrence Radiation Laboratory, (Technical Information Division), P. O. Box 808, Livermore, Calif
- 1 University of California Lawrence Radiation Laboratory, (Technical Info Div, ATTN: Dr. R. K. Wakerling), Berkeley 4, Calif
- 1 Argonne National Laboratory (Tech Library), Argonne, Ill
- 1 Oak Ridge National Laboratory (Tech Library), Oak Ridge, Tenn
- 1 Manager, Albuquerque Operations Office, US Atomic Energy Commission, P. O. Box 5400, Albuquerque, NM (Office of Manufacturing, Mr. Hugh Kay)

OTHER

- 1 Langley Research Center (NASA), Langley Fld, Hampton, Va
- 1 Office of Assistant Secretary of Defense (Civil Defense), Wash 25, DC
- 1 Institute for Defense Analysis, Room 2B257, The Pentagon, Wash 25, DC
- 1 Space Technology Labs, Inc., ATTN: Information Center, Document Procurement, P. O. Box 95001, Los Angeles 45, Calif
- 1 University of Illinois, Talbot Laboratory, Room 207, Urbana, Ill
- 1 Massachusetts Institute of Technology, Department of Civil and Sanitary Engineering, ATTN: Prof R. V. Whitman, 77 Massachusetts Avenue, Cambridge, Mass. AF 29(601)-4927

DISTRIBUTION (Cont'd)

No. Cys

- 1 The University of Michigan, University Research Security
Office, Lobby 1, East Engineering Bldg., Ann Arbor, Mich
- 1 Office of Assistant Secretary of Defense (Civil Defense), Battle
Creek, Mich
- 1 University of New Mexico, AF Shock Tube Facility, Box 188,
University Station, Albuquerque, NM
- 1 Armour Research Foundation, ATTN: Dr. E. Vey, 3422 South
Dearborn St., Chicago 15, Ill. AF 29(601)-5343
- 1 National Engineering Science Co., ATTN: Dr. Soldate, 711
South Fair Oaks Ave, Pasadena, Calif AF 29(601)-5395
- 5 United Research Services, ATTN: Mr. Harold C. Mason,
1811 Trousdale Drive, Burlingame, Calif AF 29(601)-5360
- 1 University of Notre Dame, Dept. of Civil Engineering, ATTN:
Dr. H. Saxe, Notre Dame, Ind AF 29(601)-5174
- 1 Purdue University, School of Civil Engineering, ATTN: Prof
G. A. Leonards, Lafayette, Ind AF 29(601)-5204
- 1 Paul Weidlinger and Associates, 770 Lexington Ave, New York
21, NY AF 29(601)-2855
- 1 Physics International Co. ATTN: C. Godfrey, 2229 Fourth St.,
Berkeley 10, Calif AF 29(601)-5832
- 1 Northrop Corporation, Ventura Division, ATTN: J. Trulio,
1515 Rancho Conejo Blvd, Newbury Park, Calif AF 29(601)-5971
- 1 Prof A. P. Boresi, Department of Theoretical and Applied
Mechanics, 212 Talbot Laboratory, University of Illinois,
Urbana, Ill
- 1 Dr. Ralph Fadum, School of Engineering, North Carolina State
College, Raleigh, NC
- 1 Dr. Eivind Hognestad, Manager, Structural Development Section,
Portland Cement Association, 5420 Old Orchard Road, Skokie, Ill
- 1 Dr. Lydik S. Jacobsen, Agbabian-Jacobsen & Associates, 8939
South Sepulveda Blvd., Los Angeles 45, Calif
- 1 Prof Frank Kerekes, Dean of the Faculty, Michigan College of
Mining and Technology, Houghton, Mich
- 1 Prof Carl Kisslinger, St. Louis University, 3621 Olive St.,
St. Louis 8, Mo
- 1 Prof Frank E. Richart, Jr., School of Civil Engineering,
University of Michigan, Ann Arbor, Mich

DISTRIBUTION (cont'd)

No. Cys

- | | |
|---|--|
| 1 | Michigan College of Mining and Technology, ATTN: Prof.
George A. Young, Civil Engineering Department, Houghton,
Mich |
| 1 | University of Illinois, ATTN: A. Aug, 207 Talbot Laboratory,
Urbana, Ill |
| 1 | Official Record Copy (Mr. Frederick H. Peterson, WLRS) |

<p>Air Force Special Weapons Center, Kirtland AF Base, New Mexico</p> <p>Rpt. No. AFSCM-TDR-63-47. EXPERIMENTAL STUDY OF THE EFFECT OF MATERIAL PROPERTIES ON COUPLING OF EXPLOSION ENERGY. 85 p. incl illus., table, 7 refs. May 1963.</p> <p>Unclassified report</p> <p>An experimental study was made of the influence of material properties of the directly transmitted effects on explosions. Small spherical high-explosive charges were used to load a series of cylindrical blocks of fine aggregate concrete, either at the surface of a block, within a block, or at the contact surface of two blocks. Measurements were made of the variations in concrete properties, of the total impulse delivered to the block supports, of the permanent deformations and craters, and of the air-blast pressures. It was found that material properties have a major</p>	<ol style="list-style-type: none"> 1. Blast damage 2. Concretes -- effects of blast 3. High explosives 4. Rocks -- effects of blast 5. Structural materials -- effects of blast I. AFSC Project 1080, Task 108001 II. Contract AF 29(601)-5360 III. United Research Services, Burlingame, Calif IV. Kenneth Kaplan V. Secondary Rpt. No. URS 609-11 VI. In DDC collection
<p>Air Force Special Weapons Center, Kirtland AF Base, New Mexico</p> <p>Rpt. No. AFSCM-TDR-63-47. EXPERIMENTAL STUDY OF THE EFFECT OF MATERIAL PROPERTIES ON COUPLING OF EXPLOSION ENERGY. 85 p. incl illus., table, 7 refs. May 1963.</p> <p>Unclassified report</p> <p>An experimental study was made of the influence of material properties of the directly transmitted effects on explosions. Small spherical high-explosive charges were used to load a series of cylindrical blocks of fine aggregate concrete, either at the surface of a block, within a block, or at the contact surface of two blocks. Measurements were made of the variations in concrete properties, of the total impulse delivered to the block supports, of the permanent deformations and craters, and of the air-blast pressures. It was found that material properties have a major</p>	<ol style="list-style-type: none"> 1. Blast damage 2. Concretes -- effects of blast 3. High explosives 4. Rocks -- effects of blast 5. Structural materials -- effects of blast I. AFSC Project 1080, Task 108001 II. Contract AF 29(601)-5360 III. United Research Services, Burlingame, Calif IV. Kenneth Kaplan V. Secondary Rpt. No. URS 609-11 VI. In DDC collection
<p>Air Force Special Weapons Center, Kirtland AF Base, New Mexico</p> <p>Rpt. No. AFSCM-TDR-63-47. EXPERIMENTAL STUDY OF THE EFFECT OF MATERIAL PROPERTIES ON COUPLING OF EXPLOSION ENERGY. 85 p. incl illus., table, 7 refs. May 1963.</p> <p>Unclassified report</p> <p>An experimental study was made of the influence of material properties of the directly transmitted effects on explosions. Small spherical high-explosive charges were used to load a series of cylindrical blocks of fine aggregate concrete, either at the surface of a block, within a block, or at the contact surface of two blocks. Measurements were made of the variations in concrete properties, of the total impulse delivered to the block supports, of the permanent deformations and craters, and of the air-blast pressures. It was found that material properties have a major</p>	<ol style="list-style-type: none"> 1. Blast damage 2. Concretes -- effects of blast 3. High explosives 4. Rocks -- effects of blast 5. Structural materials -- effects of blast I. AFSC Project 1080, Task 108001 II. Contract AF 29(601)-5360 III. United Research Services, Burlingame, Calif IV. Kenneth Kaplan V. Secondary Rpt. No. URS 609-11 VI. In DDC collection

<p>effect on the total impulse transmitted to the material, little effect on the air blast waves, and a very large influence on the sizes and shapes of the craters produced. Although crater dimensions appeared to vary approximately as the cube root of charge weight, both the crater volume and the total impulse varied by at least a factor of two, and scaled crater depth appeared to be approximately independent of burst geometry. The compressibility, as measured by Young's modulus, appeared to have greatest effect on the impulse, while the internal shear strength and other properties reflecting the internal structure of the material had greatest effect on crater dimensions.</p>		<p>effect on the total impulse transmitted to the material, little effect on the air blast waves, and a very large influence on the sizes and shapes of the craters produced. Although crater dimensions appeared to vary approximately as the cube root of charge weight, both the crater volume and the total impulse varied by at least a factor of two, and scaled crater depth appeared to be approximately independent of burst geometry. The compressibility, as measured by Young's modulus, appeared to have greatest effect on the impulse, while the internal shear strength and other properties reflecting the internal structure of the material had greatest effect on crater dimensions.</p>	
<p>effect on the total impulse transmitted to the material, little effect on the air blast waves, and a very large influence on the sizes and shapes of the craters produced. Although crater dimensions appeared to vary approximately as the cube root of charge weight, both the crater volume and the total impulse varied by at least a factor of two, and scaled crater depth appeared to be approximately independent of burst geometry. The compressibility, as measured by Young's modulus, appeared to have greatest effect on the impulse, while the internal shear strength and other properties reflecting the internal structure of the material had greatest effect on crater dimensions.</p>		<p>effect on the total impulse transmitted to the material, little effect on the air blast waves, and a very large influence on the sizes and shapes of the craters produced. Although crater dimensions appeared to vary approximately as the cube root of charge weight, both the crater volume and the total impulse varied by at least a factor of two, and scaled crater depth appeared to be approximately independent of burst geometry. The compressibility, as measured by Young's modulus, appeared to have greatest effect on the impulse, while the internal shear strength and other properties reflecting the internal structure of the material had greatest effect on crater dimensions.</p>	

<p>Air Force Special Weapons Center, Kirtland AF Base, New Mexico Rpt. No. AFSMC-TDR-63-47. EXPERIMENTAL STUDY OF THE EFFECT OF MATERIAL PROPERTIES ON COUPLING OF EXPLOSION ENERGY. 85 p. incl illus., table, 7 refs. May 1963.</p> <p>Unclassified report</p> <p>An experimental study was made of the influence of material properties of the directly transmitted effects on explosions. Small spherical high-explosive charges were used to load a series of cylindrical blocks of fine aggregate concrete, either at the surface of a block, within a block, or at the contact surface of two blocks. Measurements were made of the variations in concrete properties, of the total impulse delivered to the block supports, of the permanent deformations and craters, and of the air-blast pressures. It was found that material properties have a major</p>	<ol style="list-style-type: none"> 1. Blast damage 2. Concretes -- effects of blast 3. High explosives 4. Rocks -- effects of blast 5. Structural materials -- effects of blast I. AFSC Project 1080, Task 108001 II. Contract AF 29(601)-5360 III. United Research Services, Burlingame, Calif IV. Kenneth Kaplan Secondary Rpt. No. URS 609-11 VI. In DDC collection 	<p>Air Force Special Weapons Center, Kirtland AF Base, New Mexico Rpt. No. AFMWC-TDR-63-47. EXPERIMENTAL STUDY OF THE EFFECT OF MATERIAL PROPERTIES ON COUPLING OF EXPLOSION ENERGY. 85 p. incl illus., table, 7 refs. May 1963.</p> <p>Unclassified report</p> <p>An experimental study was made of the influence of material properties of the directly transmitted effects on explosions. Small spherical high-explosive charges were used to load a series of cylindrical blocks of fine aggregate concrete, either at the surface of a block, within a block, or at the contact surface of two blocks. Measurements were made of the variations in concrete properties, of the total impulse delivered to the block supports, of the permanent deformations and craters, and of the air-blast pressures. It was found that material properties have a major</p>	<ol style="list-style-type: none"> 1. Blast damage 2. Concretes -- effects of blast 3. High explosives 4. Rocks -- effects of blast 5. Structural materials -- effects of blast I. AFSC Project 1080, Task 108001 II. Contract AF 29(601)-5360 III. United Research Services, Burlingame, Calif IV. Kenneth Kaplan Secondary Rpt. No. URS 609-11 VI. In DDC collection
<p>Air Force Special Weapons Center, Kirtland AF Base, New Mexico Rpt. No. AFSMC-TDR-63-47. EXPERIMENTAL STUDY OF THE EFFECT OF MATERIAL PROPERTIES ON COUPLING OF EXPLOSION ENERGY. 85 p. incl illus., table, 7 refs. May 1963.</p> <p>Unclassified report</p> <p>An experimental study was made of the influence of material properties of the directly transmitted effects on explosions. Small spherical high-explosive charges were used to load a series of cylindrical blocks of fine aggregate concrete, either at the surface of a block, within a block, or at the contact surface of two blocks. Measurements were made of the variations in concrete properties, of the total impulse delivered to the block supports, of the permanent deformations and craters, and of the air-blast pressures. It was found that material properties have a major</p>	<ol style="list-style-type: none"> 1. Blast damage 2. Concretes -- effects of blast 3. High explosives 4. Rocks -- effects of blast 5. Structural materials -- effects of blast I. AFSC Project 1080, Task 108001 II. Contract AF 29(601)-5360 III. United Research Services, Burlingame, Calif IV. Kenneth Kaplan Secondary Rpt. No. URS 609-11 VI. In DDC collection 	<p>Air Force Special Weapons Center, Kirtland AF Base, New Mexico Rpt. No. AFSMC-TDR-63-47. EXPERIMENTAL STUDY OF THE EFFECT OF MATERIAL PROPERTIES ON COUPLING OF EXPLOSION ENERGY. 85 p. incl illus., table, 7 refs. May 1963.</p> <p>Unclassified report</p> <p>An experimental study was made of the influence of material properties of the directly transmitted effects on explosions. Small spherical high-explosive charges were used to load a series of cylindrical blocks of fine aggregate concrete, either at the surface of a block, within a block, or at the contact surface of two blocks. Measurements were made of the variations in concrete properties, of the total impulse delivered to the block supports, of the permanent deformations and craters, and of the air-blast pressures. It was found that material properties have a major</p>	<ol style="list-style-type: none"> 1. Blast damage 2. Concretes -- effects of blast 3. High explosives 4. Rocks -- effects of blast 5. Structural materials -- effects of blast I. AFSC Project 1080, Task 108001 II. Contract AF 29(601)-5360 III. United Research Services, Burlingame, Calif IV. Kenneth Kaplan Secondary Rpt. No. URS 609-11 VI. In DDC collection

<p>effect on the total impulse transmitted to the material, little effect on the air blast waves, and a very large influence on the sizes and shapes of the craters produced. Although crater dimensions appeared to vary approximately as the cube root of charge weight, both the crater volume and the total impulse varied by at least a factor of two, and scaled crater depth appeared to be approximately independent of burst geometry. The compressibility, as measured by Young's modulus, appeared to have greatest effect on the impulse, while the internal shear strength and other properties reflecting the internal structure of the material had the greatest effect on crater dimensions.</p>		<p>effect on the total impulse transmitted to the material, little effect on the air blast waves, and a very large influence on the sizes and shapes of the craters produced. Although crater dimensions appeared to vary approximately as the cube root of charge weight, both the crater volume and the total impulse varied by at least a factor of two, and scaled crater depth appeared to be approximately independent of burst geometry. The compressibility, as measured by Young's modulus, appeared to have greatest effect on the impulse, while the internal shear strength and other properties reflecting the internal structure of the material had the greatest effect on crater dimensions.</p>	
<p>effect on the total impulse transmitted to the material, little effect on the air blast waves, and a very large influence on the sizes and shapes of the craters produced. Although crater dimensions appeared to vary approximately as the cube root of charge weight, both the crater volume and the total impulse varied by at least a factor of two, and scaled crater depth appeared to be approximately independent of burst geometry. The compressibility, as measured by Young's modulus, appeared to have greatest effect on the impulse, while the internal shear strength and other properties reflecting the internal structure of the material had the greatest effect on crater dimensions.</p>		<p>effect on the total impulse transmitted to the material, little effect on the air blast waves, and a very large influence on the sizes and shapes of the craters produced. Although crater dimensions appeared to vary approximately as the cube root of charge weight, both the crater volume and the total impulse varied by at least a factor of two, and scaled crater depth appeared to be approximately independent of burst geometry. The compressibility, as measured by Young's modulus, appeared to have greatest effect on the impulse, while the internal shear strength and other properties reflecting the internal structure of the material had the greatest effect on crater dimensions.</p>	